Supplementary Information

Carpatizine, a Novel Bridged Oxazine Derivative Generated by Non-enzymatic Reaction

Peng Fu and John B. MacMillan*

Department of Biochemistry, University of Texas Southwestern Medical Center at Dallas, Dallas, Texas 75390, United States

List of Supplementary Information

Experimental Details

General Experimental Procedures. Optical rotations were recorded with an AUTOPOL AP IV-6W polarimeter equipped with a halogen lamp (589 nm). UV spectra were recorded on a Shimadzu UV-1601 UV–VIS spectrophotometer. ECD spectra were measured on JASCO J-815 spectrometer. IR spectra were obtained on a Perkin Elmer Spectrum 1000 FT-IR Spectrometer. ^{1}H and 2D NMR spectroscopic data were recorded at 600 MHz in CD_3OD or $CDCl_3$ solution on Varian System spectrometer, and chemical shifts were referenced to the corresponding residual solvent signal ($\delta_{H/C}$ 3.31/49.00 for CD_3OD and $\delta_{H/C}$ 7.26/77.16 for $CDCl_3$). ^{13}C NMR spectra were acquired at 100 MHz on a Varian System spectrometer. High resolution ESI-TOF mass spectra were provided by The Scripps Research Institute, La Jolla, CA. Low-resolution LC/ESI-MS data were measured using an Agilent 1200 series LC/MS system with a reversed-phase EVO C_{18} column (Phenomenex Kinetex, 100 mm × 4.6 mm, 2.6 μm) at a flow rate of 0.7 mL/min. Preparative HPLC was performed on an Agilent 1200 series instrument with a DAD detector, using a reversed-phase C_{18} column (Phenomenex Luna, 250 × 10.0 mm, 5 μm), a C_8 column (Phenomenex Luna, 250 × 10.0 mm, 5 μm), or a phenyl-hexyl column (Phenomenex Luna, 250 × 10.0 mm, 5 μm). Sephadex LH-20 (GE Healthcare) and ODS (50 mm, Merck) were used for column chromatography. Artificial seawater was used in microbial fermentations as described in a previous reference.[S1]

Collection and Phylogenetic Analysis of Strain SNE-011. The actinomycete *Streptomyces* sp. SNE-011 was isolated as previously described.[S2]

Cultivation and Extraction of SNE-011. Details of the method are the same as our previous report.[S2]

Purification. The extract (3.9 g) was partitioned with EtOAc/H_2O. The EtOAc soluble layer (1.6 g) was

fractionated by flash column chromatography on ODS (50 μm, 30 g), eluting with a step gradient of MeOH and H_2O (10:90–100:0), and 11 fractions (Fr.1–Fr.11) were collected. Fractions 4 (49.0 mg) was separated into eight fractions (Fr.4.1–Fr.4.8) on Sephadex LH-20, eluting with MeOH. Fr.4.3 (5.1 mg) was purified by HPLC on a C_{18} column (Phenomenex Luna, 250 × 10.0 mm, 5 μm, 2.5 mL/min) using a gradient solvent system from 10% to 65% CH_3CN (0.1% formic acid) over 20 min to afford compound **1** (0.9 mg, t_R = 14.9 min).

*Carpatizine (**1**):* colorless oil, $[\alpha]_D^{23}$ –78 (*c* 0.1, MeOH); UV (MeOH) λ_{max} (log ε): 298 (4.11) nm; ECD (*c* 0.8 mM, MeOH) λ_{max} ($\Delta\varepsilon$) 326 (+0.2), 265 (–4.0), 218 (+6.5) nm; IR (NaCl disk) ν_{max}: 3334, 2954, 1634, 1594, 1358, 1280, 1164, 1101, 1049, 994, 880 cm^{-1}; ^1H and ^{13}C NMR, Table 1; HRESIMS *m/z* 365.2071 $[M + H]^+$ (calcd for $C_{19}H_{29}N_2O_5$, 365.2071).

Methylation of 1. To a solution of **1** (2.0 mg) in DMF (anhydrous, 0.5 mL) was added 10.0 mg of NaH. After allowing it to stir at 0 ℃ for 0.5 h, 50 μL of CH_3I was added into the reaction mixture. It was stirred at room temperature for another 2 h. Then, a saturated solution of NH_4Cl (2.0 mL) was added to quench the reaction. The product was extracted with CH_2Cl_2 (2 × 10.0 mL) and purified by reversed-phase HPLC (Phenomenex Luna, C_8, 250 × 10.0 mm, 2.5 mL/min, 5 μm) using a gradient solvent system from 20% to 100% CH_3CN (0.1% formic acid) over 20 min to afford compound **1a** (1.9 mg, t_R = 15.9 min, 83% yield). Compound **1a**, colorless oil; ^1H NMR (600 MHz, $CDCl_3$) δ 6.96 (1H, dd, *J* = 15.5, 10.9 Hz, H-3′), 6.10 (1H, dd, *J* = 14.9, 11.0 Hz, H-4′), 5.92 (1H, dt, *J* = 15.0, 7.5 Hz, H-5′), 5.78 (1H, d, *J* = 15.5 Hz, H-2′), 5.72 (1H, s, H-6), 4.67 (1H, dd, *J* = 2.9, 1.5 Hz, H-3), 3.86 (1H, d, *J* = 1.5 Hz, H-4), 3.76 (1H, d, *J* = 2.9 Hz, H-2), 3.56 (3H, s, 2-OCH_3), 3.52 (3H, s, 4-OCH_3), 3.48 (3H, s, 5-OCH_3), 2.98 (3H, s, 9-NCH_3), 2.93 (3H, s, 9-NCH_3), 2.44 (4H, m, H-7&H-8), 2.01 (2H, dd, *J* = 7.5, 6.7 Hz, H-6′), 1.66 (1H, m, H-7′), 0.88 (6H, d, *J* = 6.7 Hz, H-8′& H-9′); ^{13}C NMR (100 MHz, $CDCl_3$) δ 172.2 (C-9), 154.9 (C-1′), 140.1 (C-5′), 138.5 (C-3′), 136.9 (C-1), 130.3 (C-4′), 128.9 (C-6), 122.5 (C-2′), 84.1 (C-5), 81.6 (C-2), 72.9 (C-3), 71.2 (C-4), 59.9 (2-OCH_3), 58.0 (4-OCH_3), 50.1 (5-OCH_3), 42.4 (C-6′), 37.4 (9-NCH_3), 35.7 (9-NCH_3), 31.8 (C-8), 28.6 (C-7′), 28.2 (C-8), 22.4 (C-8′&C-9′); HRESIMS *m/z* 421.2695 $[M + H]^+$ (calcd for $C_{23}H_{37}N_2O_5$, 421.2697).

Chemical Transformation from Daryamide D (2) to Carpatizine (1) and Carpatamides E and F (3 and 4). Daryamide D (**2**, 10.0 mg) was dissolved in 2.0 mL of methanol, and 37% HCl (20 μL) was then added. The reaction mixture was stirred for 1 h at room temperature (rt). Then, the mixture was evaporated to give the reaction product, which was further purified by reversed-phase HPLC (Phenomenex Luna, C_8, 250 × 10.0 mm, 2.5 mL/min, 5 μm) using a gradient solvent system from 10% to 65% CH_3CN (0.1% formic acid) over 20 min to afford a pure compound (5.9 mg, t_R = 14.4 min, 57% yield). This product was identified as same as compound **1** by LC-MS, NMR, and specific rotation. The rest from HPLC was got together and further purified by reversed-phase HPLC (Phenomenex Luna, phenyl-hexyl, 250 × 10.0 mm, 2.5 mL/min, 5 μm) using 35% CH_3CN (0.1% formic acid) to afford compounds **3** (1.4 mg, t_R = 37.0 min, 15% yield) and **4** (0.9 mg, t_R = 38.8 min, 9% yield). The structures of **3** and **4** were elucidated by comparison of NMR data with known compounds, carpatamides A and B (Figure 4 and Table S1).[S2]

Chemical Transformation of Daryamide D (2) at High Temperature. Daryamide D (**2**, 50.0 mg) was dissolved in 5.0 mL of dioxane. The reaction mixture was stirred at 220 ℃ in a sealed glass tube for 2 h. Then, the mixture was evaporated to give the reaction product, which was separated into six fractions (Fr.1–Fr.6) by flash column chromatography on ODS (50 μm, 30 g), eluting with a step gradient of MeOH and H_2O (10:90–100:0). Fr.4 (21.8 mg) was purified by reversed-phase HPLC (Phenomenex Luna, C_{18}, 250 × 10.0 mm, 2.5 mL/min, 5 μm) using 75% CH_3CN (0.1% formic acid) to afford Fr.4-1 (11.9 mg, t_R = 6.6 min), compounds **5** (2.2 mg, t_R = 7.5 min) and **6** (1.6 mg, t_R = 8.1 min). Fr.4-1 was further purified by reversed-phase HPLC (Phenomenex Luna, phenyl-hexyl, 250 ×

10.0 mm, 2.5 mL/min, 5 μm) using 35% CH_3CN (0.1% formic acid) to afford compounds **3** (5.6 mg, t_R = 37.0 min) and **4** (2.6 mg, t_R = 38.8 min). Fr.6 (10.4 mg) was purified by reversed-phase HPLC (Phenomenex Luna, C_{18}, 250 × 10.0 mm, 2.5 mL/min, 5 μm) using 80% CH_3CN (0.1% formic acid) to afford compounds **7** (3.0 mg, t_R = 7.7 min) and **8** (2.7 mg, t_R = 8.6 min). The structures of new compounds **6** and **8** were elucidated by comparison of NMR data with compounds **3** and **4**, and the analysis of their HRESIMS data (Figure 4 and Table S1).

*Carpatamide E (**3**):* yellow oil; ^1H and ^{13}C NMR, Table S1; HRESIMS *m/z* 333.1809 $[M + H]^+$ (calcd for $C_{18}H_{25}N_2O_4$, 333.1809).

*Carpatamide F (**4**):* yellow oil; ^1H and ^{13}C NMR, Table S1; HRESIMS *m/z* 333.1808 $[M + H]^+$ (calcd for $C_{18}H_{25}N_2O_4$, 333.1809).

*Carpatamide G (**6**):* yellow oil; ^1H and ^{13}C NMR, Table S1; HRESIMS *m/z* 334.1648 $[M + H]^+$ (calcd for $C_{18}H_{25}NO_5$, 334.1649).

*Carpatamide H (**8**):* yellow oil; ^1H and ^{13}C NMR, Table S1; HRESIMS *m/z* 316.1543 $[M + H]^+$ (calcd for $C_{18}H_{22}NO_4$, 316.1543).

Antibiotic Assays. The antibiotic activities against *Pseudomonas aeruginosa* and *Bacillus subtilis* were evaluated by an agar dilution method. The tested strains were cultivated in LB agar plates at 37 ℃. Compounds **1**, **3**, **4**, **6**, **8** and positive control (erythromycin) were dissolved in MeOH at different concentrations from 100 to 0.1 μg/mL by the continuous 10-fold dilution methods. A 10 μL quantity of test solution was absorbed by a paper disk (5 mm diameter) and placed on the assay plates. After 24 h incubation, zones of inhibition (mm in diameter) were recorded.

Cytotoxicity Assays. Cell lines were cultivated in 10 cm dishes (Corning, Inc.) in NSCLC cell-culture medium: RPMI/L-glutamine medium (Invitrogen, Inc.), 1000 U/mL penicillin (Invitrogen, Inc.), 1 mg/mL streptomycin (Invitrogen, Inc.), and 5% fetal bovine serum (Atlanta Biologicals, Inc.). Cell lines were grown in a humidified environment in the presence of 5% CO_2 at 37 ℃. For cell viability assays, HCC366, A549, HCC44 and H2122 cells (60 μL) were plated individually at a density of 1200, 750 and 500 cells/well, respectively, in 384-well microtiter assay plates (Bio-one; Greiner, Inc.). After incubating the assay plates overnight under the growth conditions described above, purified compounds were dissolved and diluted in DMSO and subsequently added to each plate with final compound concentrations ranging from 50 μM to 1 nM and a final DMSO concentration of 0.5%. After an incubation of 96 h under growth conditions, Cell Titer Glo reagent (Promega, Inc.) was added to each well (10 mL of a 1:2 dilution in NSCLC culture medium) and mixed. Plates were incubated for 10 min at room temperature, and luminescence was determined for each well using an Envision multimodal plate reader (Perkin-Elmer, Inc.). Relative luminescence units were normalized to the untreated control wells (cells plus DMSO only). Data were analyzed using the Assay Analyzer and Condoseo modules of the Screener Software Suite (GeneData, Inc.) as described previously.[S3]

Theory and Calculation Details. The calculations were performed by using the density functional theory (DFT) as carried out in the Gaussian 03.[S4] The preliminary conformational distributions search was performed by HyperChem 7.5 software. All ground-state geometries were optimized at the B3LYP/6-31G(d) level. Solvent effects of methanol solution were evaluated at the same DFT level by using the SCRF/PCM method.[S5] TDDFT[S6] at B3LYP/6-31G(d) was employed to calculate the electronic excitation energies and rotational strengths in methanol.

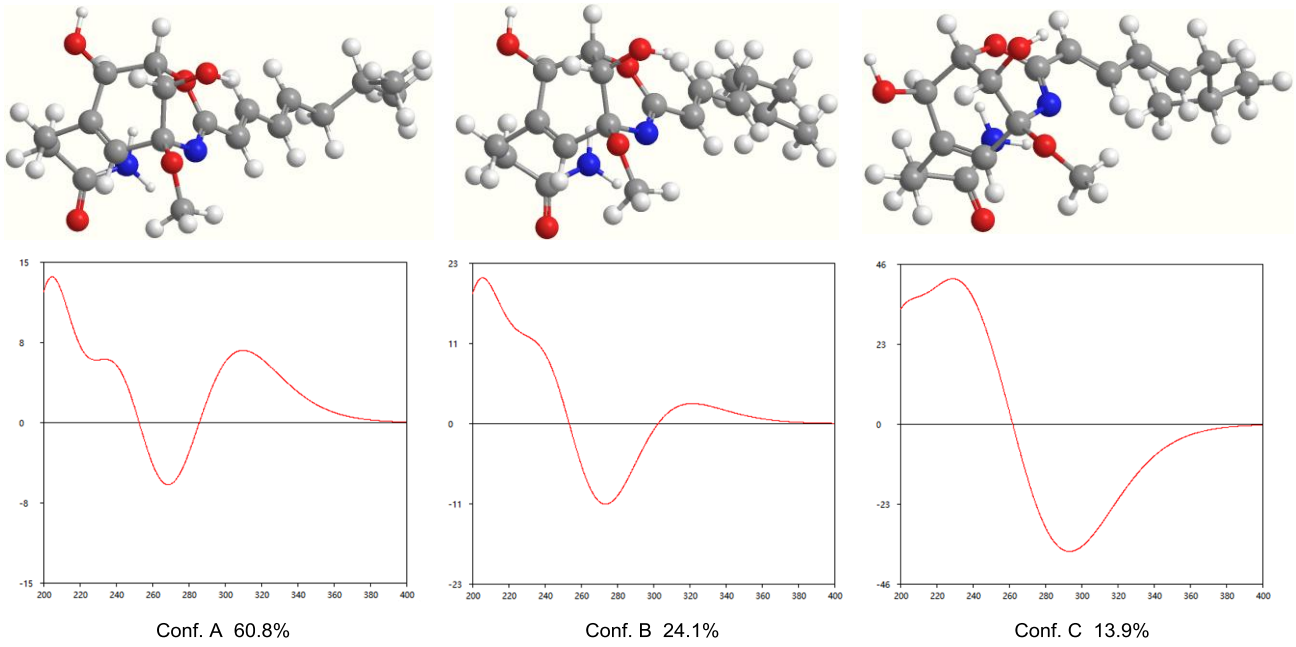

Figure S1. DFT optimized geometries of the three lowest-energy conformers of (2*R*, 3*S*, 4*S*, 5*S*)-**1**, and their individual calculated ECD spectra.

References:

(S1) M. D. Keller, R. C. Selvin, W. Claus and R. R. L. Guillard, *J. Phycol.*, 1987, **23**, 633−638.

(S2) P. Fu, M. Johnson, H. Chen, B. A. Posner and J. B. MacMillan, *J. Nat. Prod.*, 2014, **77**, 1245–1248.

(S3) H. S. Kim, S. Mendiratta, J. Kim, C. V. Pecot, J. E. Larsen, I. Zubovych, B. Y. Seo, J. Kim, B. Eskiocak, H. Chung, E. McMillan, S. Wu, J. De Brabander, K. Komurov, J. E. Toombs, S. Wei, M. Peyton, N. Williams, A. F. Gazdar, B. A. Posner, R. A. Brekken, A. K. Sood, R. J. Deberardinis, M. G. Roth, J. D. Minna and M. A. White, *Cell*, 2013, **155**, 552–566.

(S4) Gaussian 03, Revision E.01, M. J. Frisch, G. W. Trucks, H. B. Schlegel, G. E. Scuseria, M. A. Robb, J. R. Cheeseman, J. A. Montgomery, Jr., T. Vreven, K. N. Kudin, J. C. Burant, J. M. Millam, S. S. Iyengar, J. Tomasi, V. Barone, B. Mennucci, M. Cossi, G. Scalmani, N. Rega, G. A. Petersson, H. Nakatsuji, M. Hada, M. Ehara, K. Toyota, R. Fukuda, J. Hasegawa, M. Ishida, T. Nakajima, Y. Honda, O. Kitao, H. Nakai, M. Klene, X. Li, J. E. Knox, H. P. Hratchian, J. B. Cross, V. Bakken, C. Adamo, J. Jaramillo, R. Gomperts, R. E. Stratmann, O. Yazyev, A. J. Austin, R. Cammi, C. Pomelli, J. W. Ochterski, P. Y. Ayala, K. Morokuma, G. A. Voth, P. Salvador, J. J. Dannenberg, V. G. Zakrzewski, S. Dapprich, A. D. Daniels, M. C. Strain, O. Farkas, D. K. Malick, A. D. Rabuck, K. Raghavachari, J. B. Foresman, J. V. Ortiz, Q. Cui, A. G. Baboul, S. Clifford, J. Cioslowski, B. B. Stefanov, G. Liu, A. Liashenko, P. Piskorz, I. Komaromi, R. L. Martin, D. J. Fox, T. Keith, M. A. Al-Laham, C. Y. Peng, A. Nanayakkara, M. Challacombe, P. M. W. Gill, B. Johnson, W. Chen, M. W. Wong, C. Gonzalez and J. A. Pople, Gaussian, Inc., Wallingford CT, 2004.

(S5) (a) S. Miertus and J. Tomasi, *Chem. Phys.*, 1982, **65**, 239–245. (b) J. Tomasi and M. Persico, *Chem. Rev.*, 1994, **94**, 2027–2094. (c) R. Cammi and J. Tomasi, *J. Comp. Chem.*, 1995, **16**, 1449–1458.

(S6) (a) M. E. Casida, In Recent Advances in Density Functional Methods, part I; D. P. Chong, Eds.; World Scientific: Singapore, 1995; pp 155–192. (b) E. K. U. Gross, J. F. Dobson and M. Petersilka, *Top. Curr. Chem.*, 1996, **181**, 81–172. (c) E. K. U. Gross and W. Kohn, *Adv. Quantum Chem.*, 1990, **21**, 255–291. (d) E. Runge and E. K. U. Gross, *Phys. Rev. Lett.*, 1984, **52**, 997–1000.

Table S1. ^{1}H (600 MHz) and ^{13}C (100 MHz) NMR Data for Compounds **3**, **4**, **6** and **8** in CD_3OD

	3		**4**		**6**		**8**	
no.	δ_C	δ_H, mult. (*J* in Hz)	δ_C	δ_H, mult. (*J* in Hz)	δ_C	δ_H, mult. (*J* in Hz)	δ_C	δ_H, mult. (*J* in Hz)
1	120.1, C		133.8, C		134.4, C		114.9, C	
2	155.0, C		113.4, CH	6.56, s	113.4, CH	6.56, s	150.5, C	
3	105.3, CH	6.37, s	148.2, C		148.2, C		105.2, CH	6.55, s
4	149.7, C		136.6, C		136.5, C		149.5, C	
5	119.1, C		127.5, C		127.5, C		123.9, C	
6	125.5, CH	7.11, s	114.2, CH	6.77, s	114.2, CH	6.73, s	122.7, CH	7.65, s
7	26.9, CH_2	2.79, t (7.4)	32.3, CH_2	2.76, t (7.6)	32.2, CH_2	2.76, t (7.5)	24.0, CH_2	2.92, t (7.6)
8	36.9, CH_2	2.48, t (7.4)	38.5, CH_2	2.45, t (7.6)	38.4, CH_2	2.50, t (7.5)	30.3, CH_2	2.76, t (7.6)
9	178.9, C		178.3, C		178.7, C		170.7, C	
1′	167.3, C		167.7, C		167.7, C		167.4, C	
2′	122.5, CH	6.16, d (14.9)	122.3, CH	6.19, d (14.9)	122.3, CH	6.19, d (14.9)	122.9, CH	6.20, d (14.7)
3′	143.4, CH	7.25, dd (14.9, 10.8)	144.1, CH	7.30, dd (14.9, 10.9)	144.1, CH	7.29, dd (14.9, 10.8)	143.6, CH	7.27, dd (14.9, 10.8)
4′	130.9, CH	6.27, dd (15.0, 10.9)	130.9, CH	6.28, dd (15.0, 10.9)	130.9, CH	6.28, dd (15.0, 10.9)	130.9, CH	6.28, dd (15.0, 10.9)
5′	143.7, CH	6.16, dt (14.9, 7.0)	144.2, CH	6.18, dt (15.0, 7.0)	144.2, CH	6.19, dt (15.0, 7.0)	143.9, CH	6.18, dt (15.0, 7.0)
6′	43.4, CH_2	2.10, dd (7.0, 7.0)	43.4, CH_2	2.10, dd (7.0, 7.0)	43.4, CH_2	2.10, dd (7.0, 7.0)	43.4, CH_2	2.10, dd (7.0, 7.0)
7′	29.6, CH	1.73, m	29.6, CH	1.73, m	29.6, CH	1.73, m	29.6, CH	1.73, m
8′	22.7, CH_3	0.94, d (6.7)	22.7, CH_3	0.94, d (6.7)	22.7, CH_3	0.94, d (6.7)	22.7, CH_3	0.94, d (6.7)
9′	22.7, CH_3	0.94, d (6.7)	22.7, CH_3	0.94, d (6.7)	22.7, CH_3	0.94, d (6.7)	22.7, CH_3	0.94, d (6.7)

Figure S2. ^{1}H-NMR spectrum of carpatizine (**1**) in CD_3OD

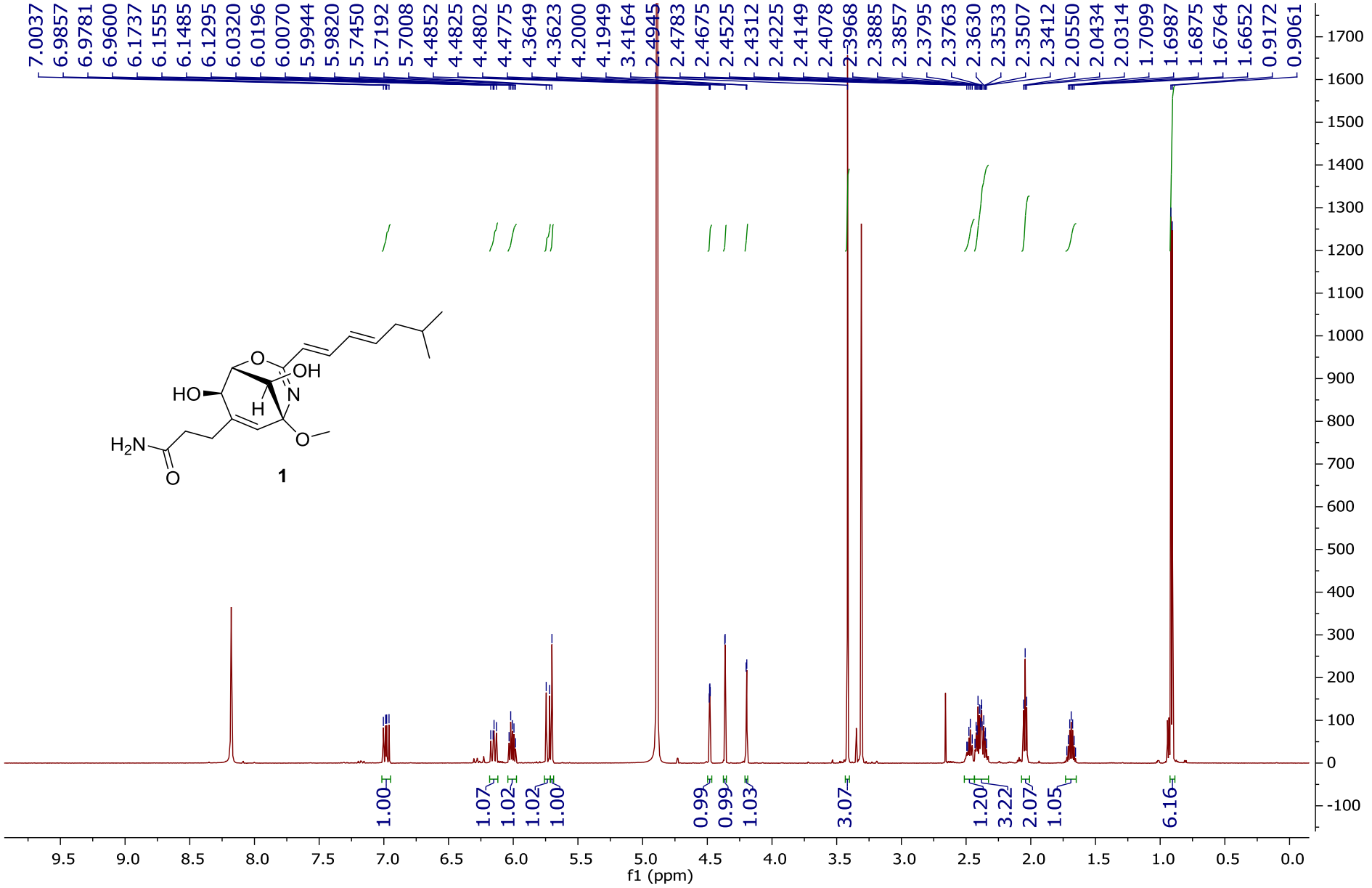

Figure S3. ^{13}C-NMR spectrum of carpatizine (**1**) in CD_3OD

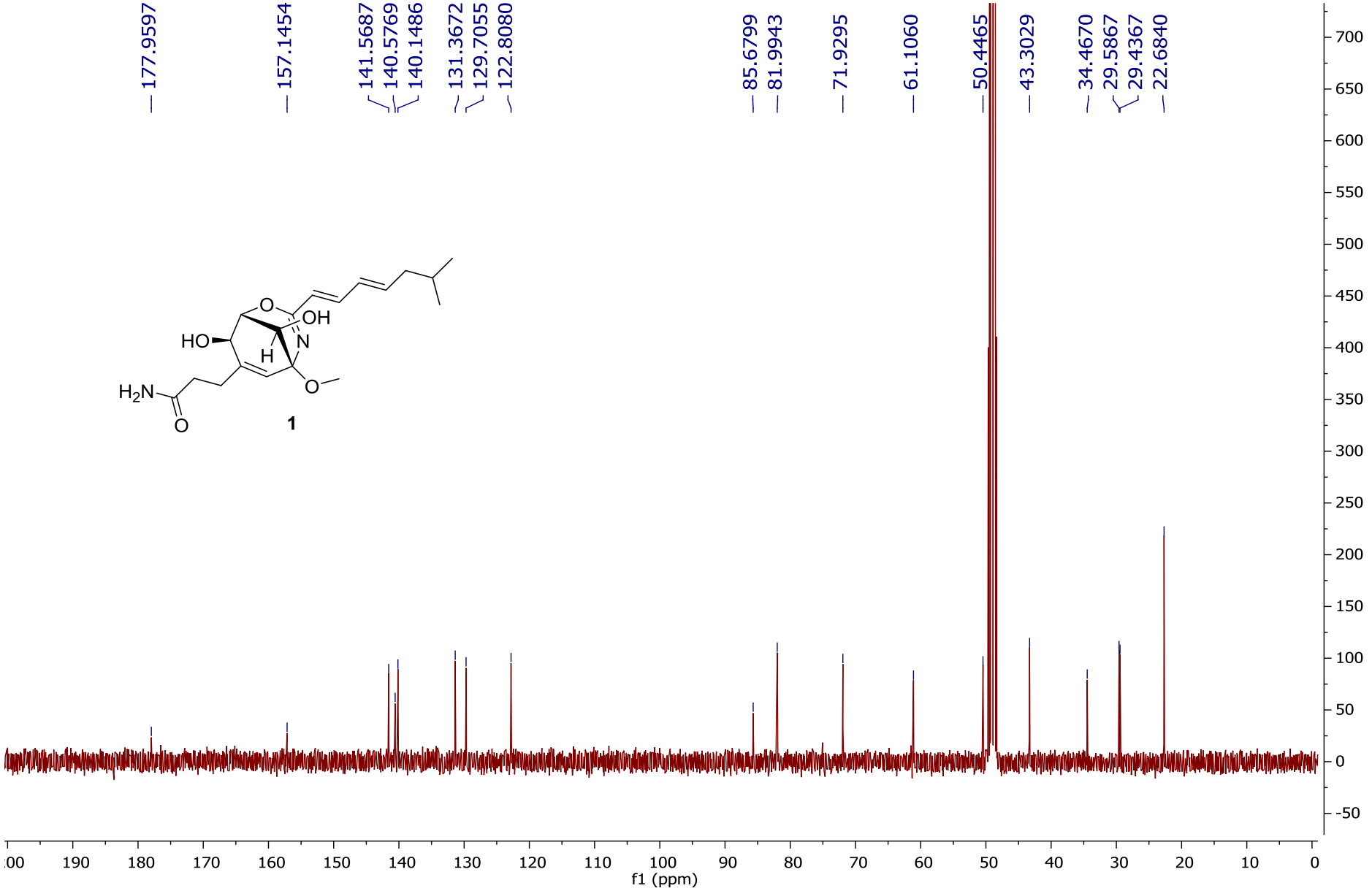

Figure S4. HSQC spectrum of carpatizine (**1**) in CD_3OD

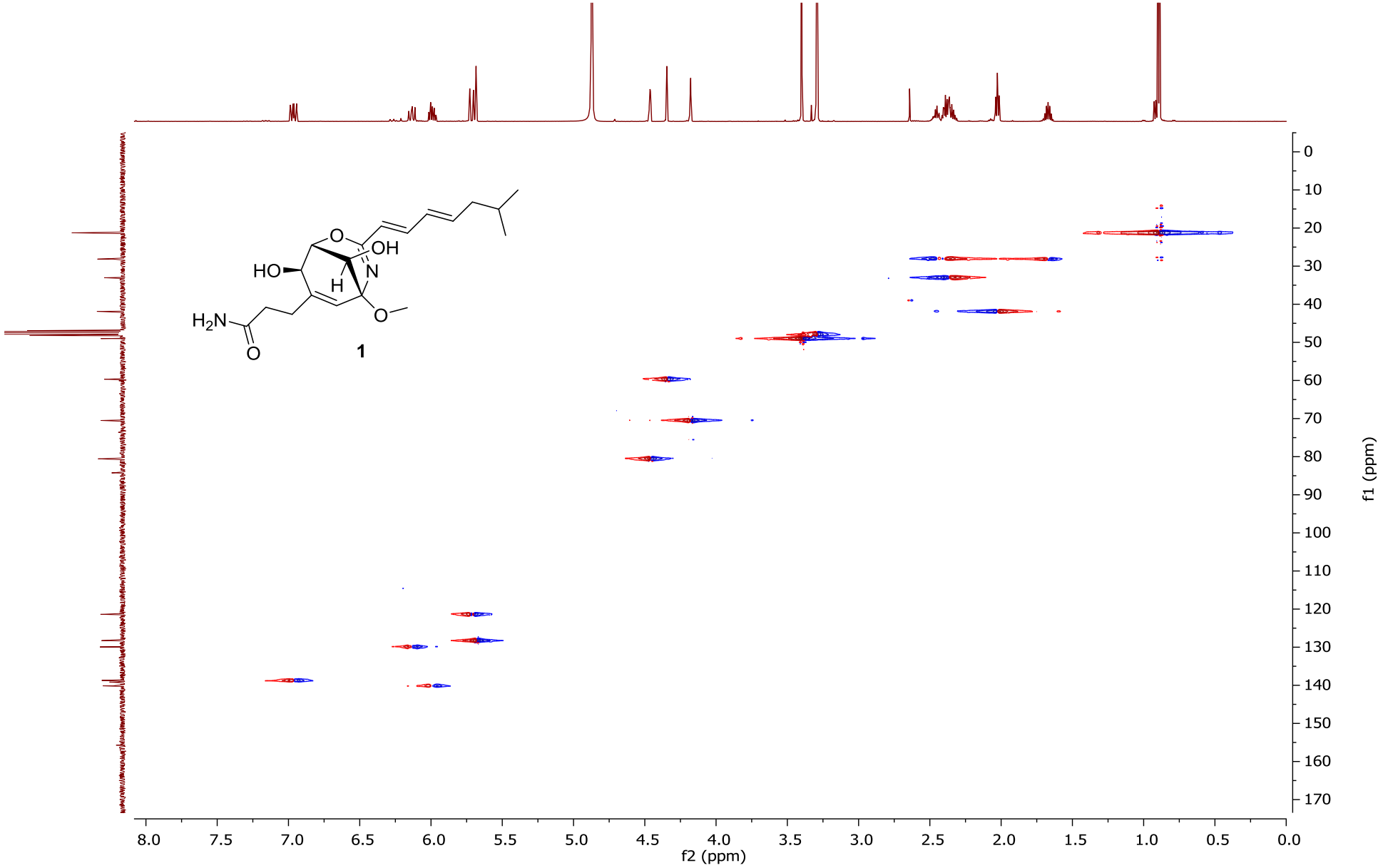

Figure S5. ^{1}H-^{1}H COSY spectrum of carpatizine (**1**) in CD_3OD

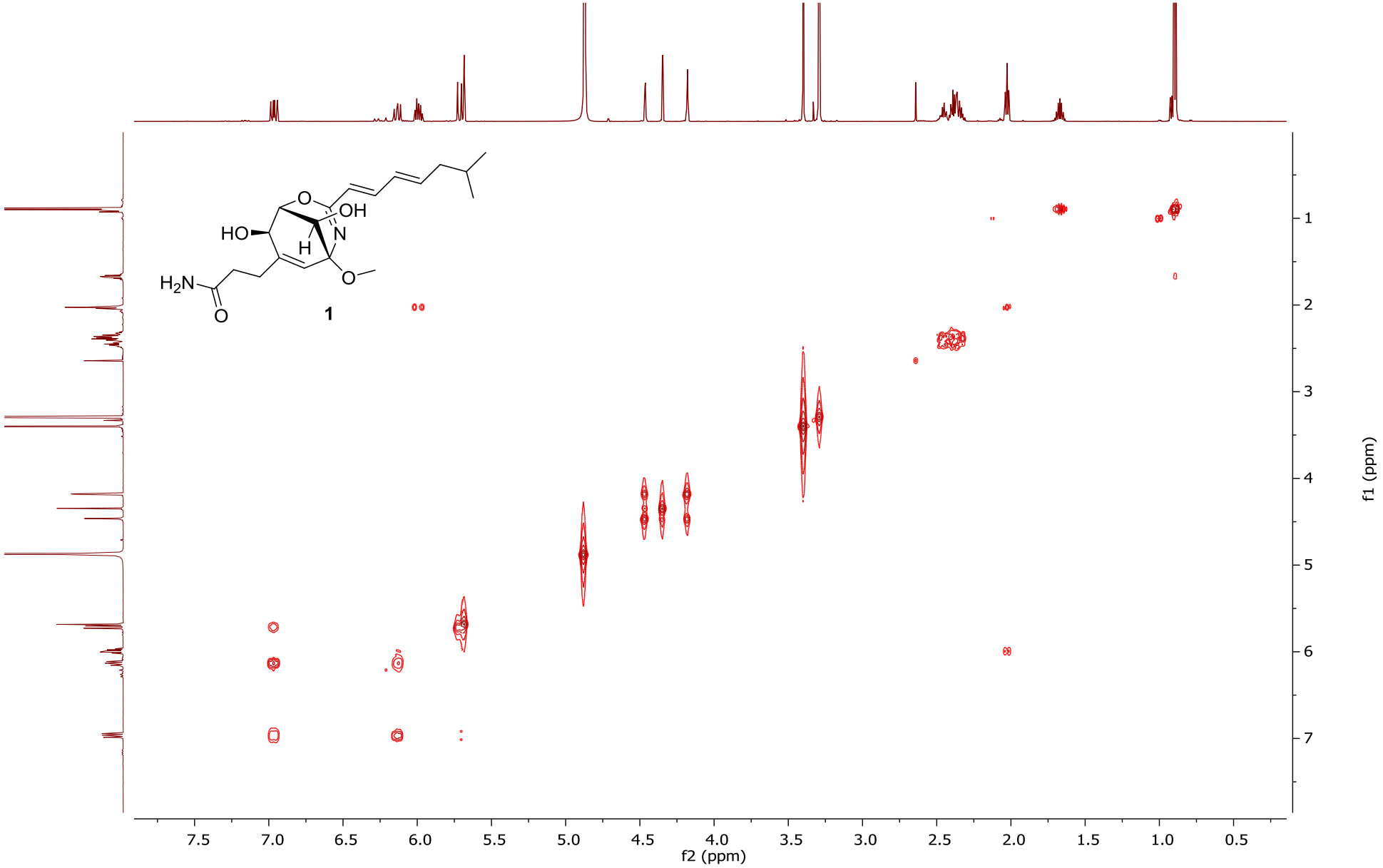

Figure S6. HMBC spectrum of carpatizine (**1**) in CD_3OD

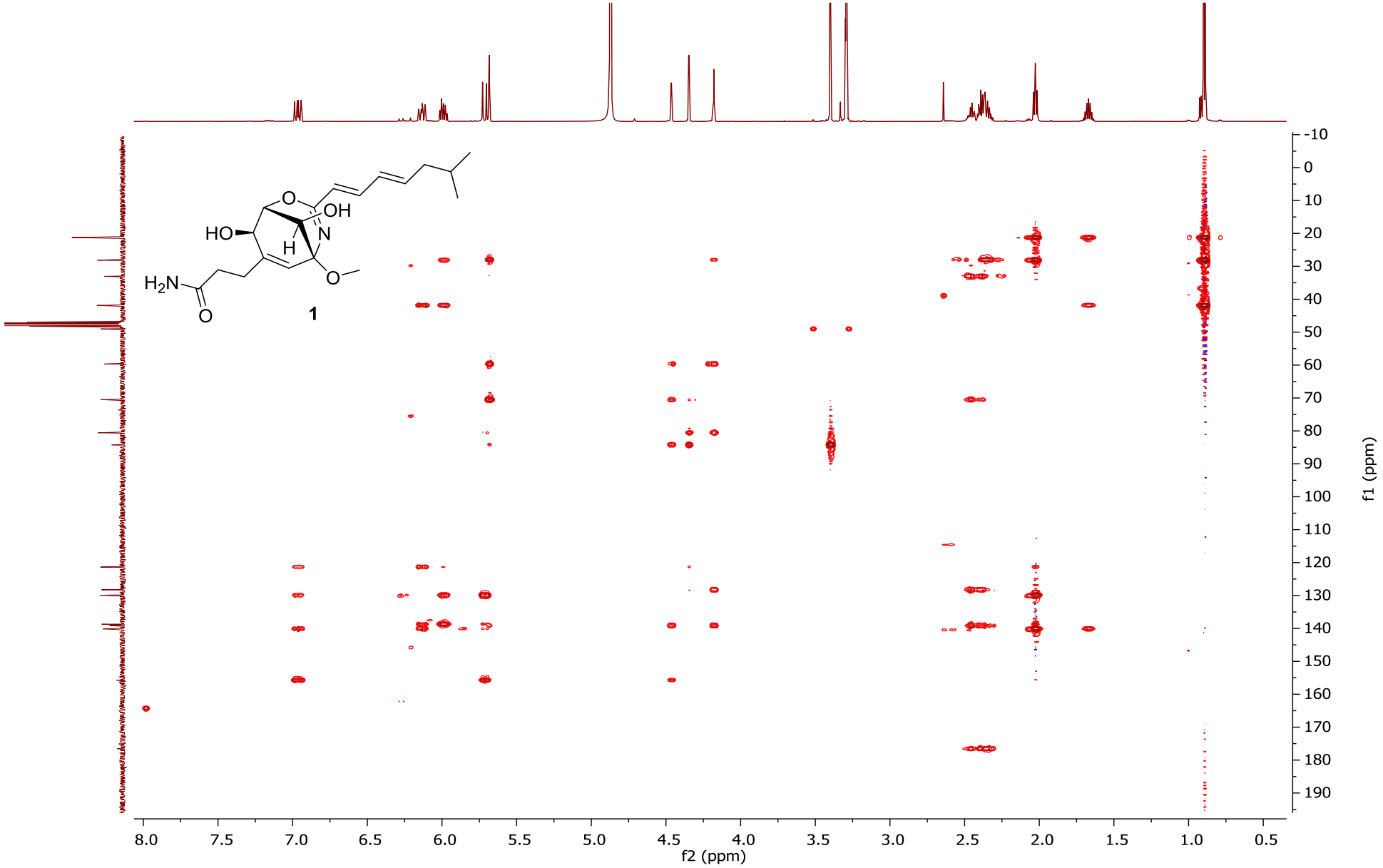

Figure S7. ^{1}H-NMR spectrum of compound **1a** in $CDCl_3$

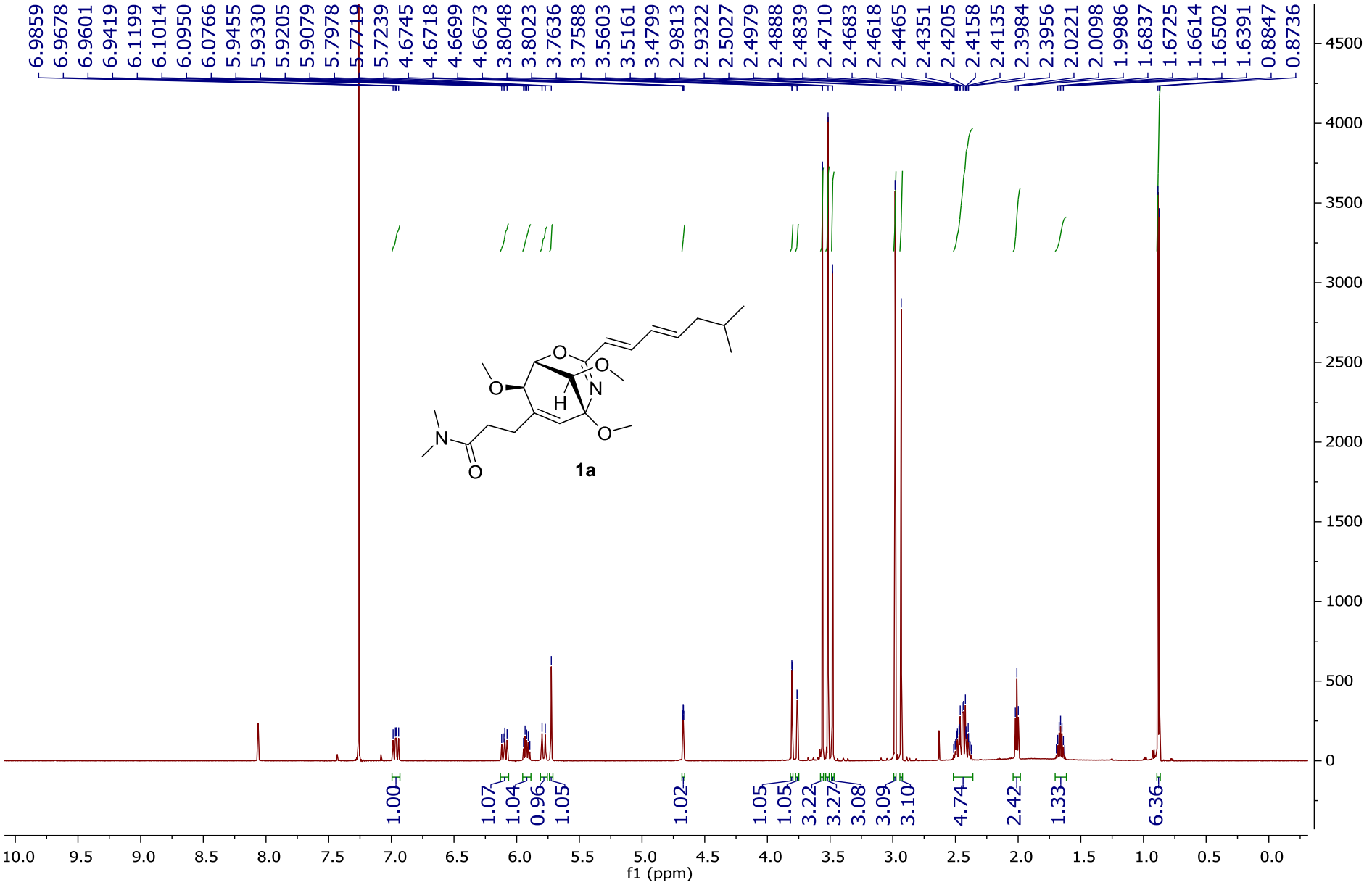

Figure S8. ^{13}C-NMR spectrum of compound **1a** in $CDCl_3$

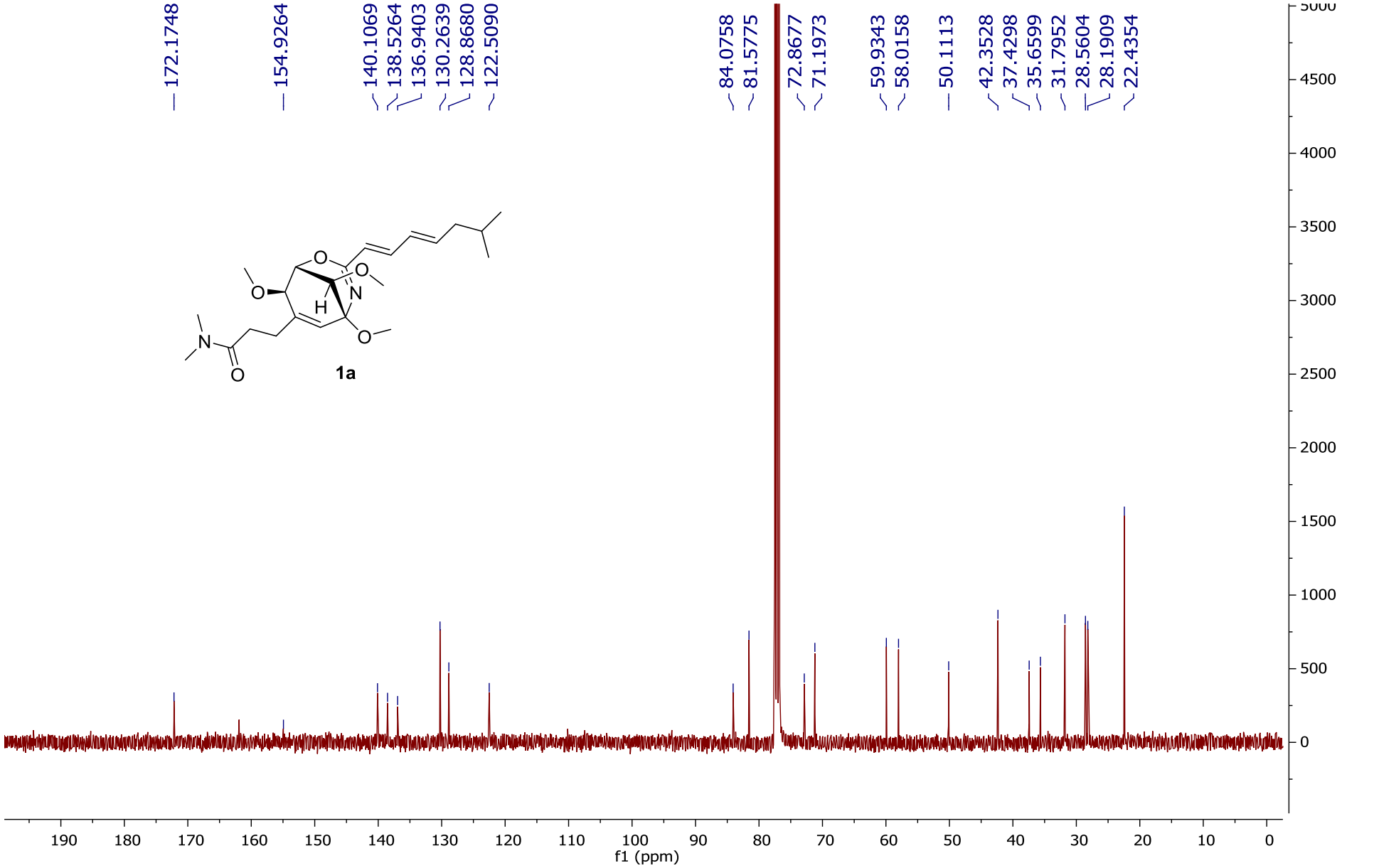

Figure S9. HSQC spectrum of compound **1a** in $CDCl_3$

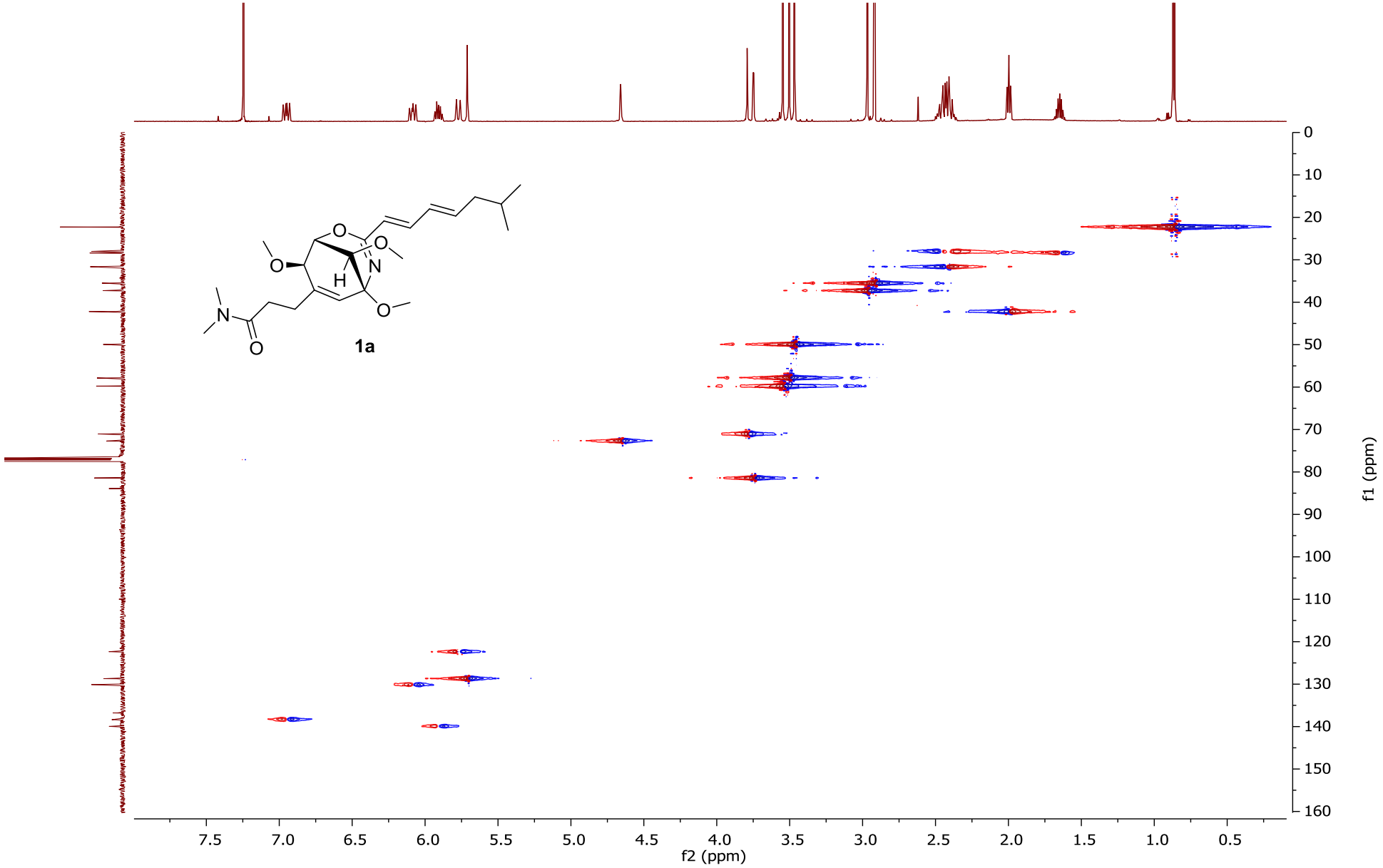

Figure S10. ^{1}H-^{1}H COSY spectrum of compound **1a** in $CDCl_3$

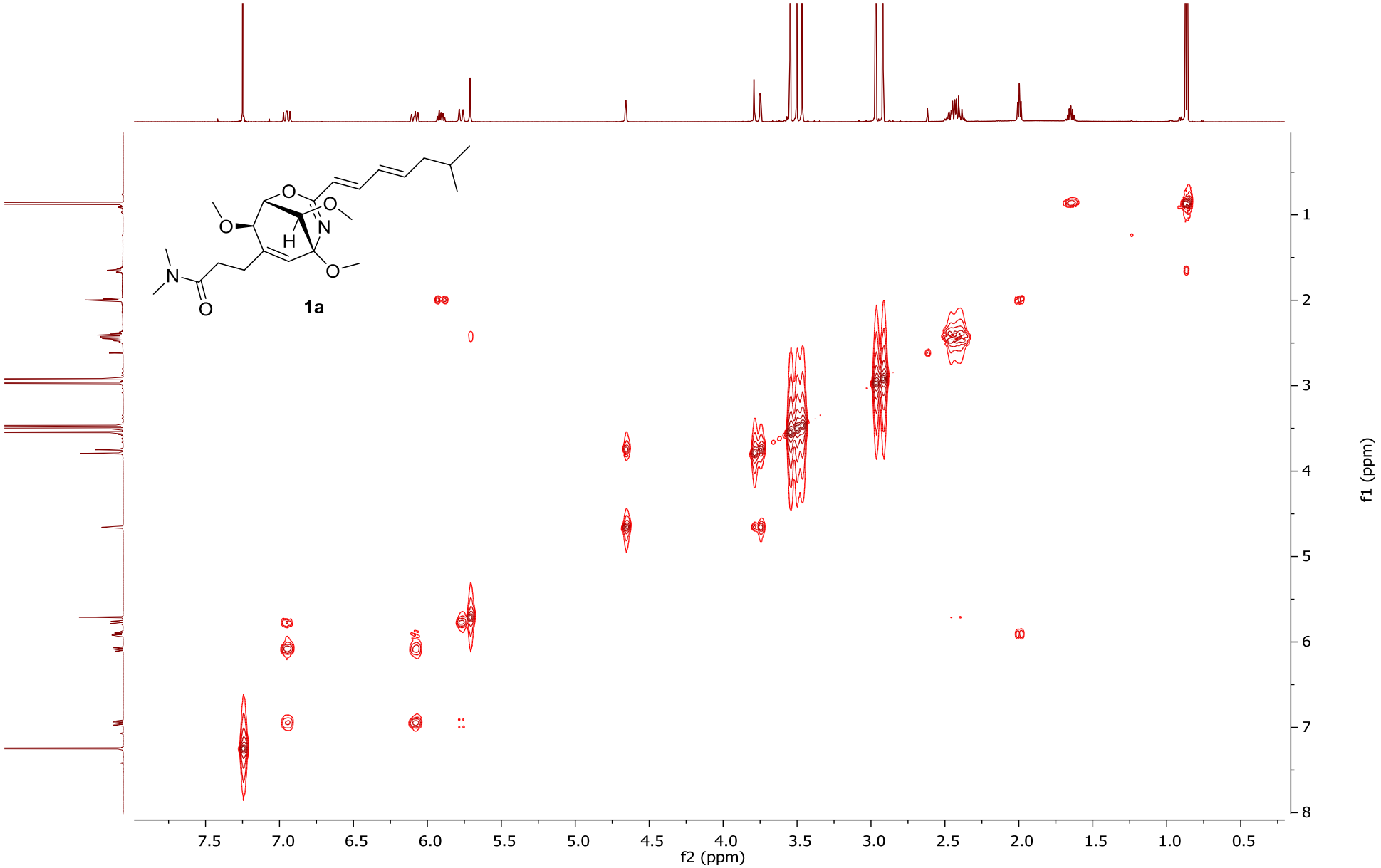

Figure S11. HMBC spectrum of compound **1a** in $CDCl_3$

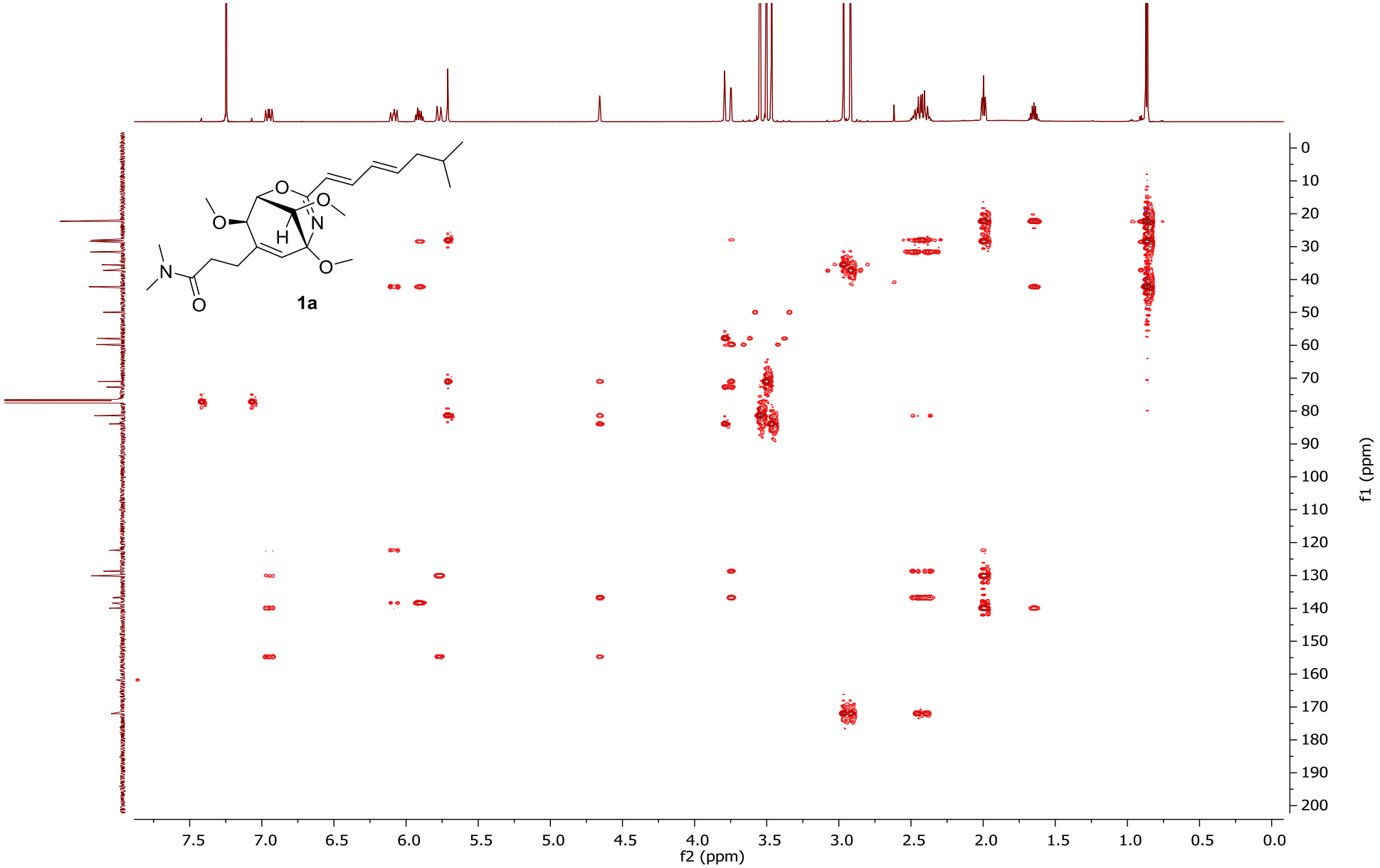

Figure S12. NOESY spectrum of compound **1a** in $CDCl_3$

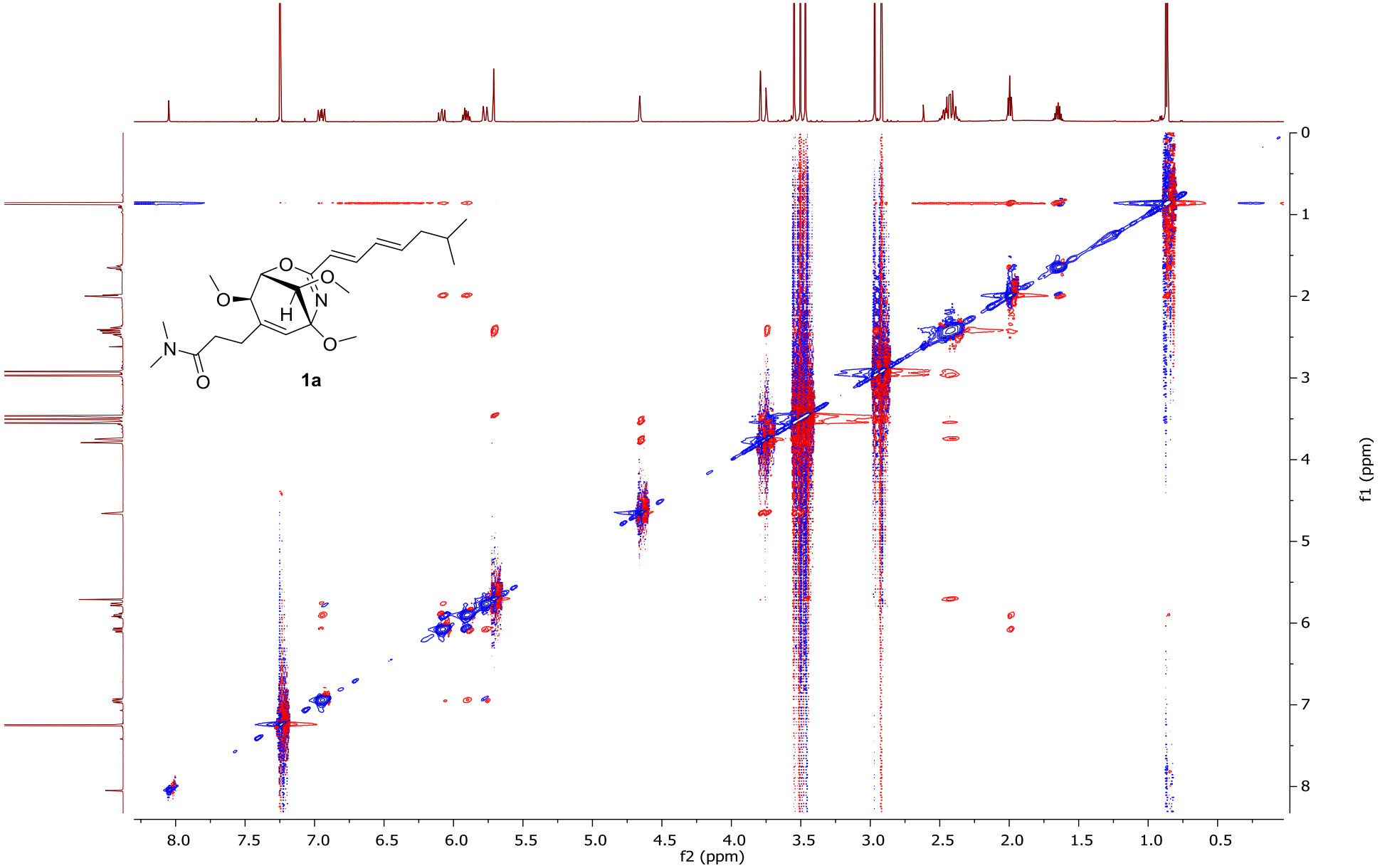

Figure S13. 1D NOE spectrum of compound **1a** in $CDCl_3$

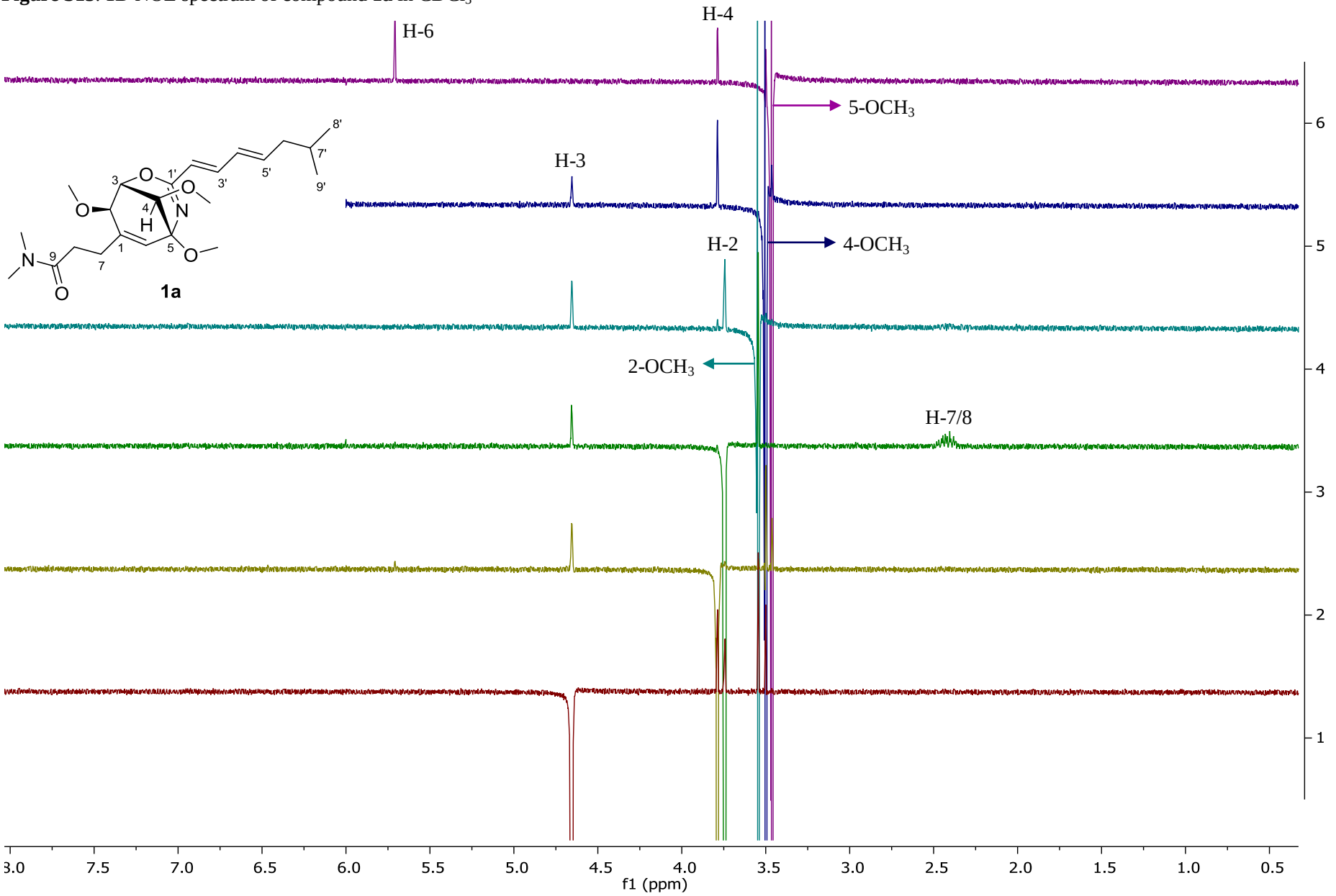

Figure S14. ^{1}H-NMR spectrum of carpatamide E (**3**) in CD_3OD

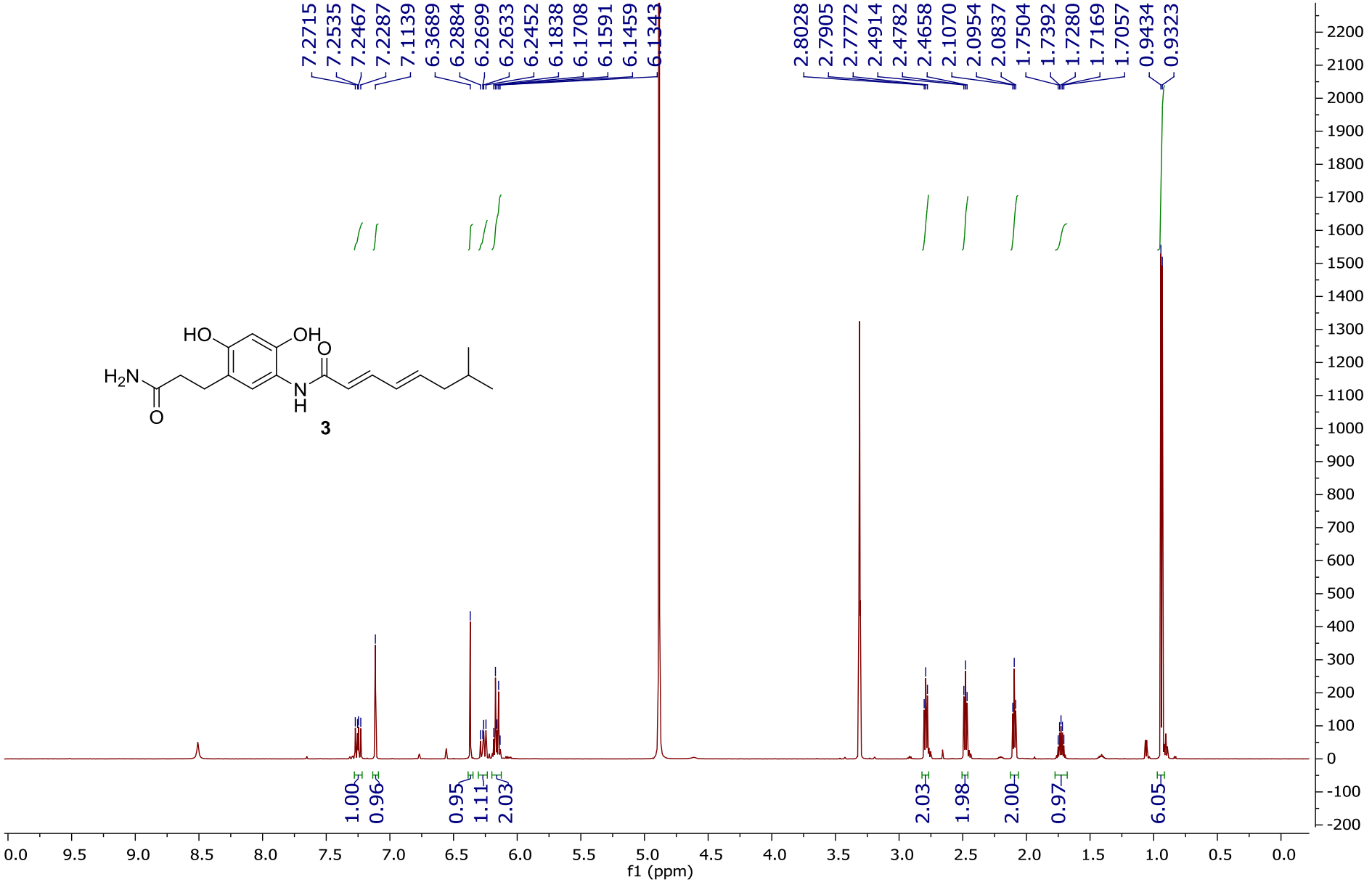

Figure S15. ^{13}C-NMR spectrum of carpatamide E (**3**) in CD_3OD

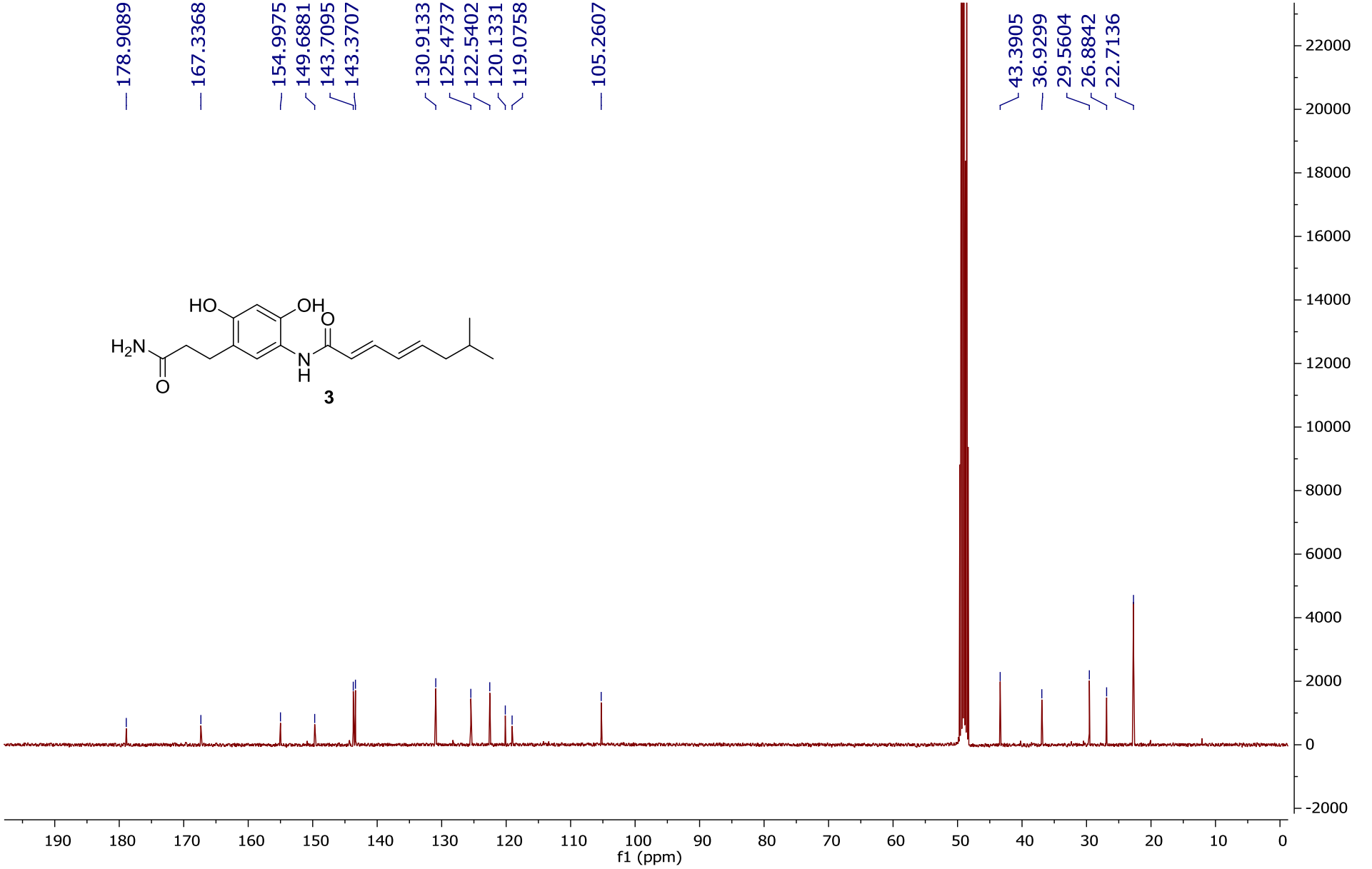

Figure S16. HSQC spectrum of carpatamide E (**3**) in CD_3OD

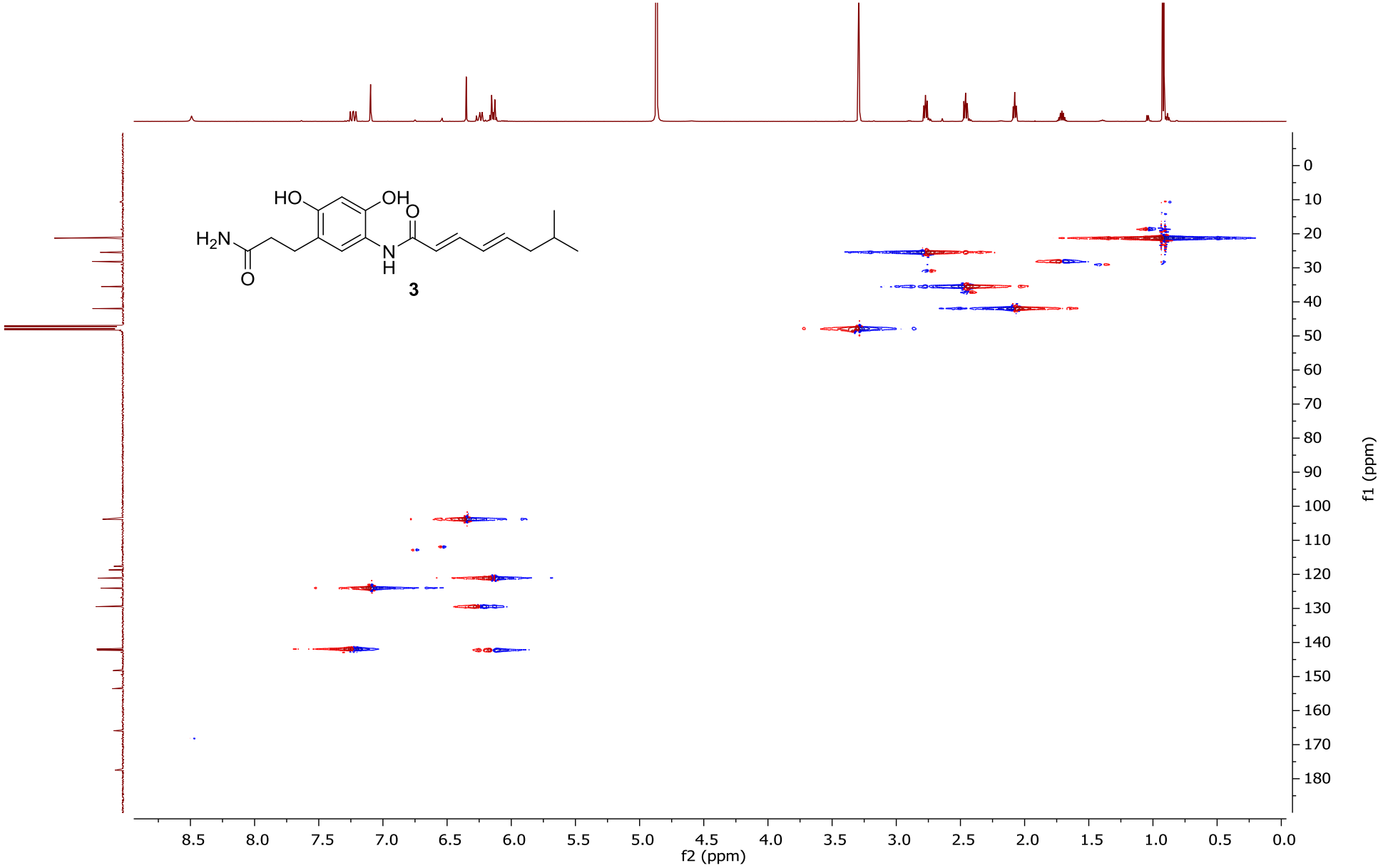

Figure S17. ^{1}H-^{1}H COSY spectrum of carpatamide E (**3**) in CD_3OD

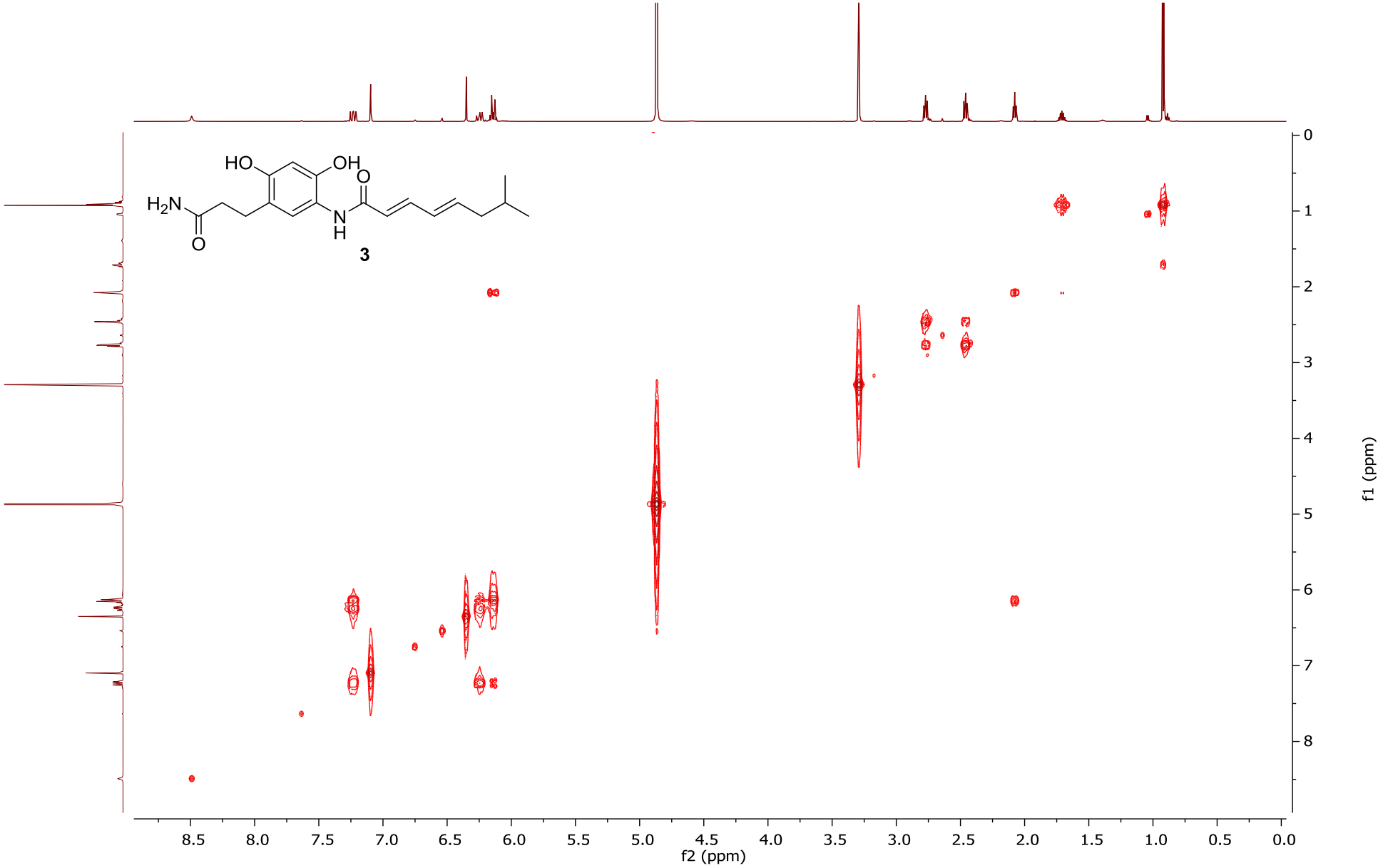

Figure S18. HMBC spectrum of carpatamide E (**3**) in CD_3OD

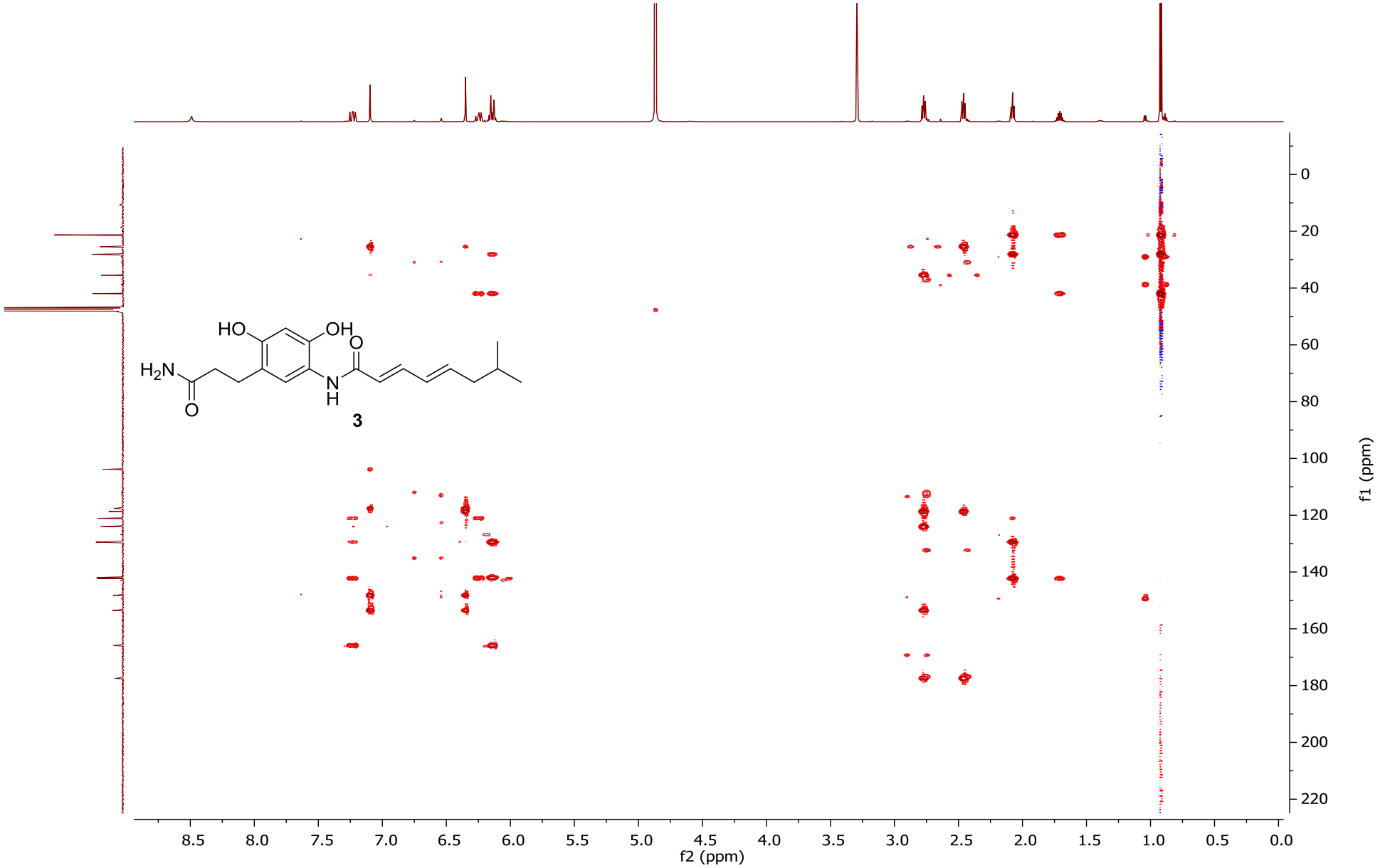

Figure S19. ^{1}H-NMR spectrum of carpatamide F (**4**) in CD_3OD

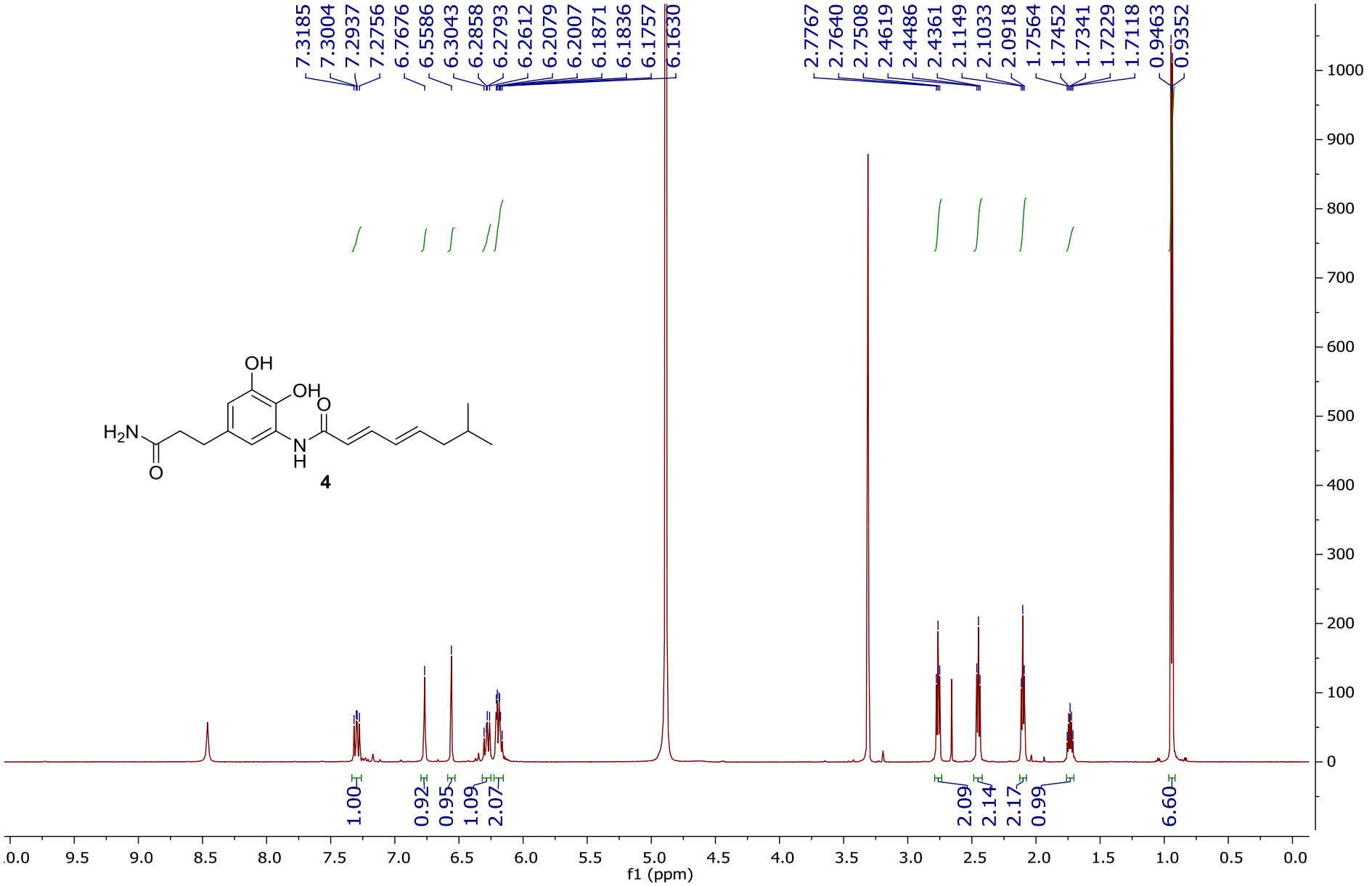

Figure S20. ^{13}C-NMR spectrum of carpatamide F (**4**) in CD_3OD

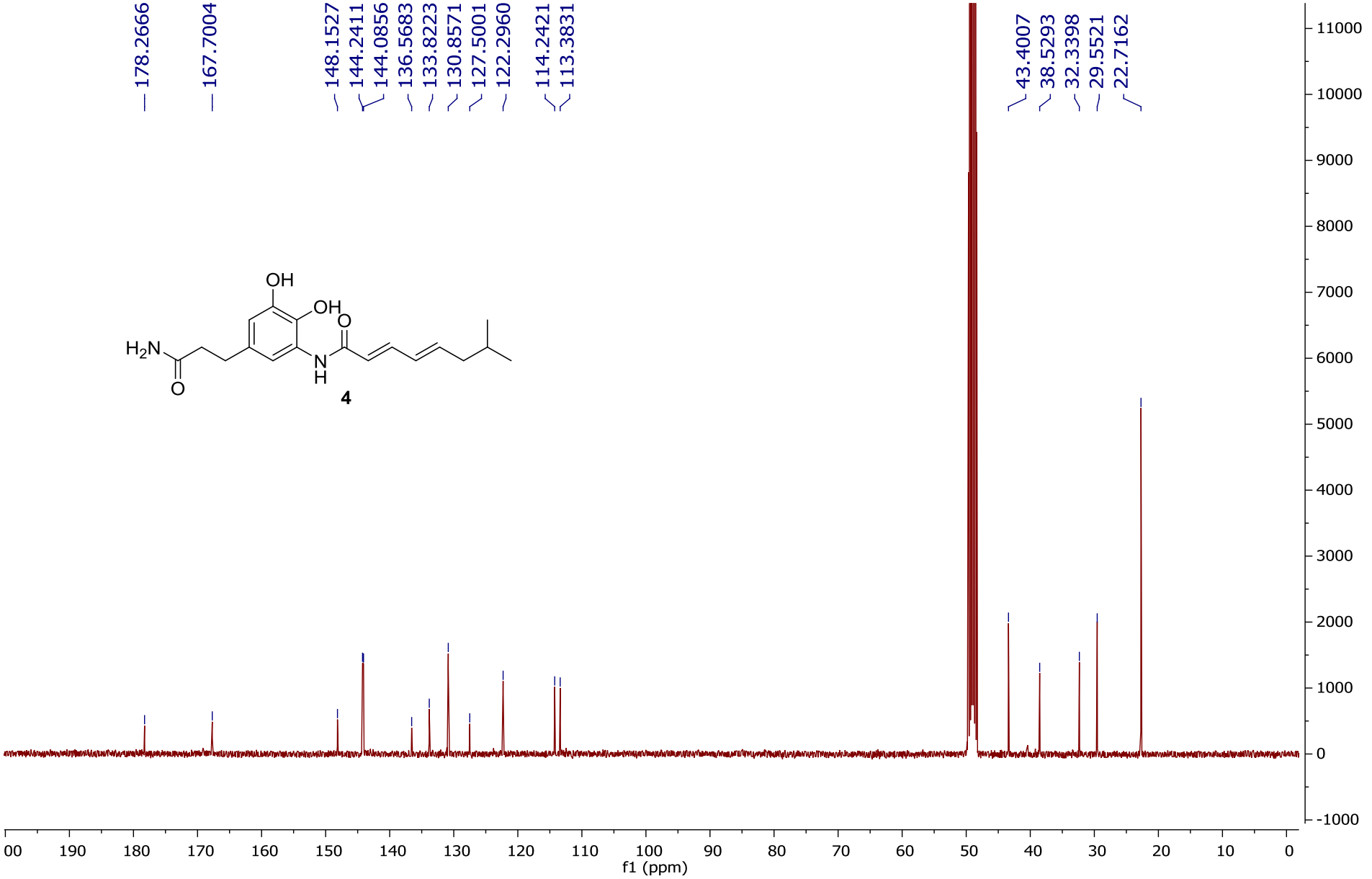

Figure S21. HSQC spectrum of carpatamide F (**4**) in CD_3OD

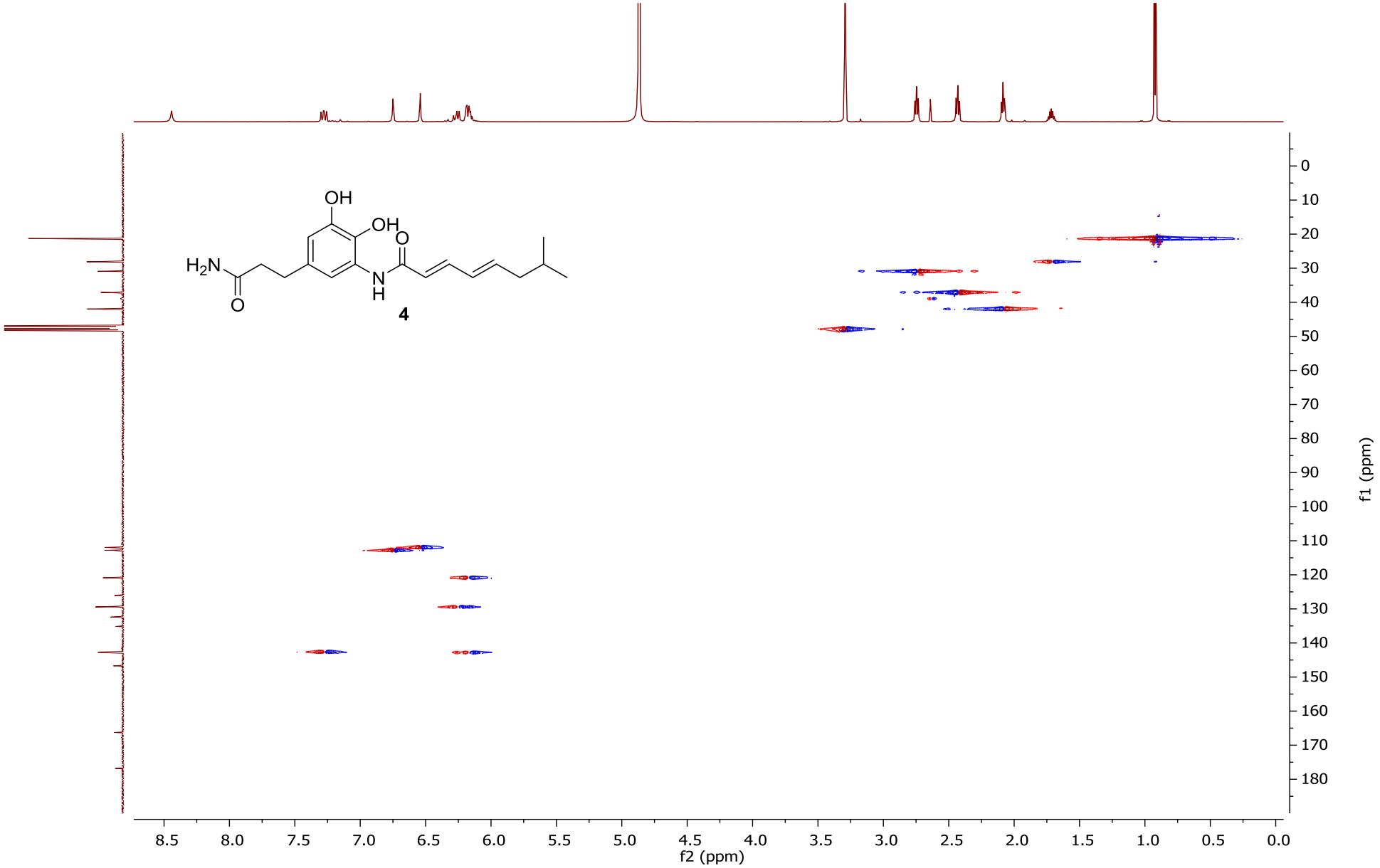

Figure S22. ^{1}H-^{1}H COSY spectrum of carpatamide F (**4**) in CD_3OD

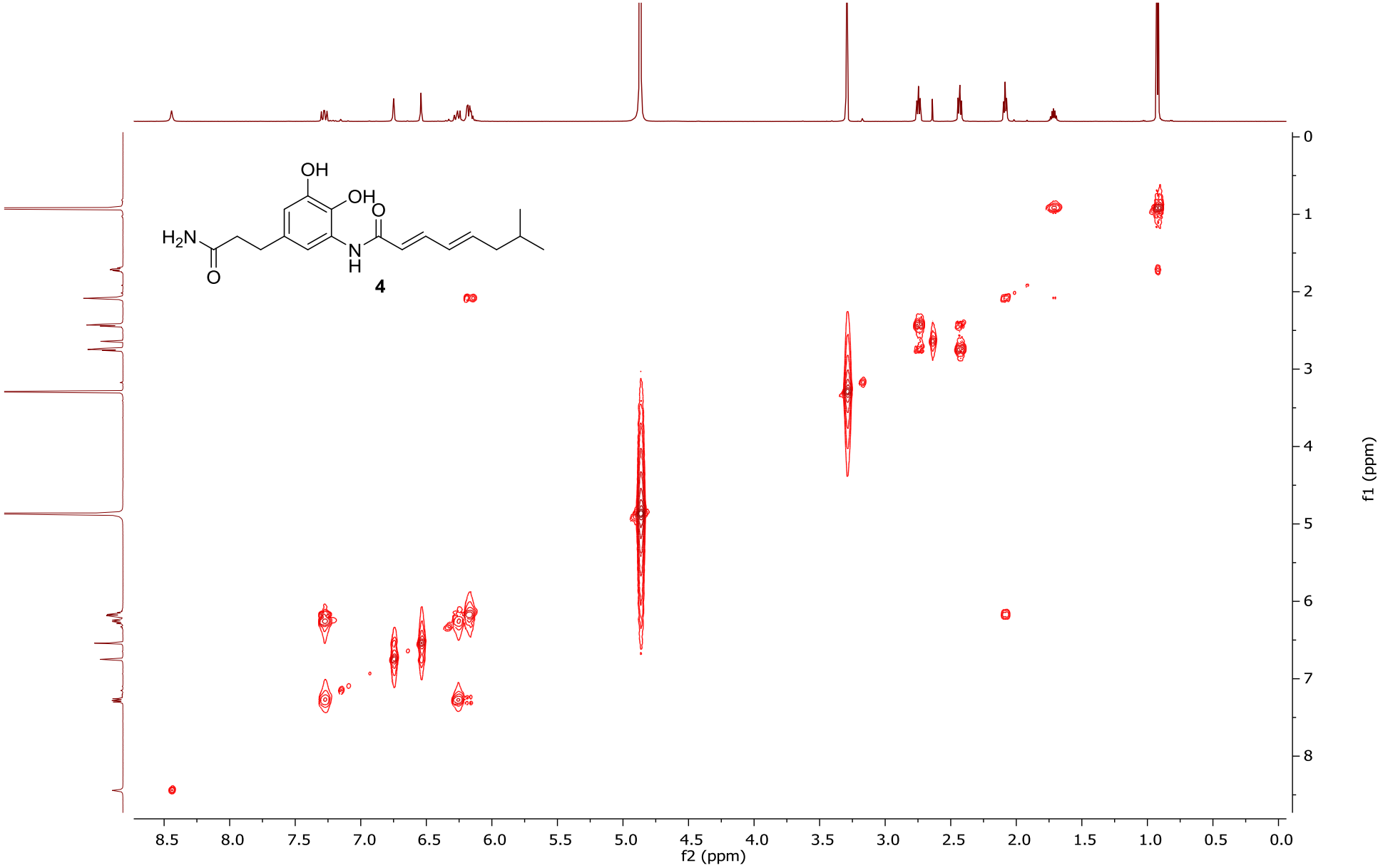

Figure S23. HMBC spectrum of carpatamide F (**4**) in CD_3OD

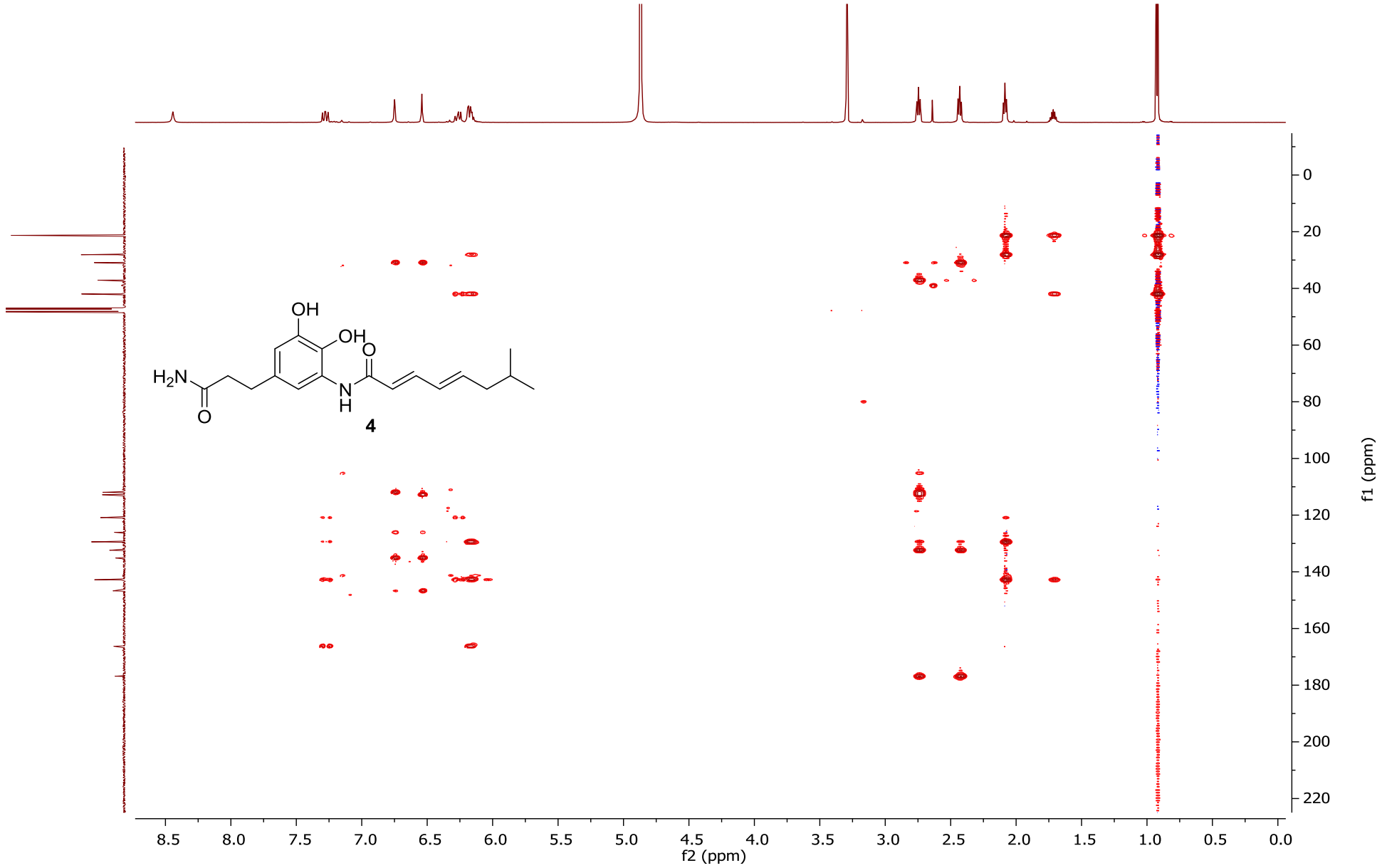

Figure S24. ^{1}H-NMR spectrum of carpatamide G (**6**) in CD_3OD

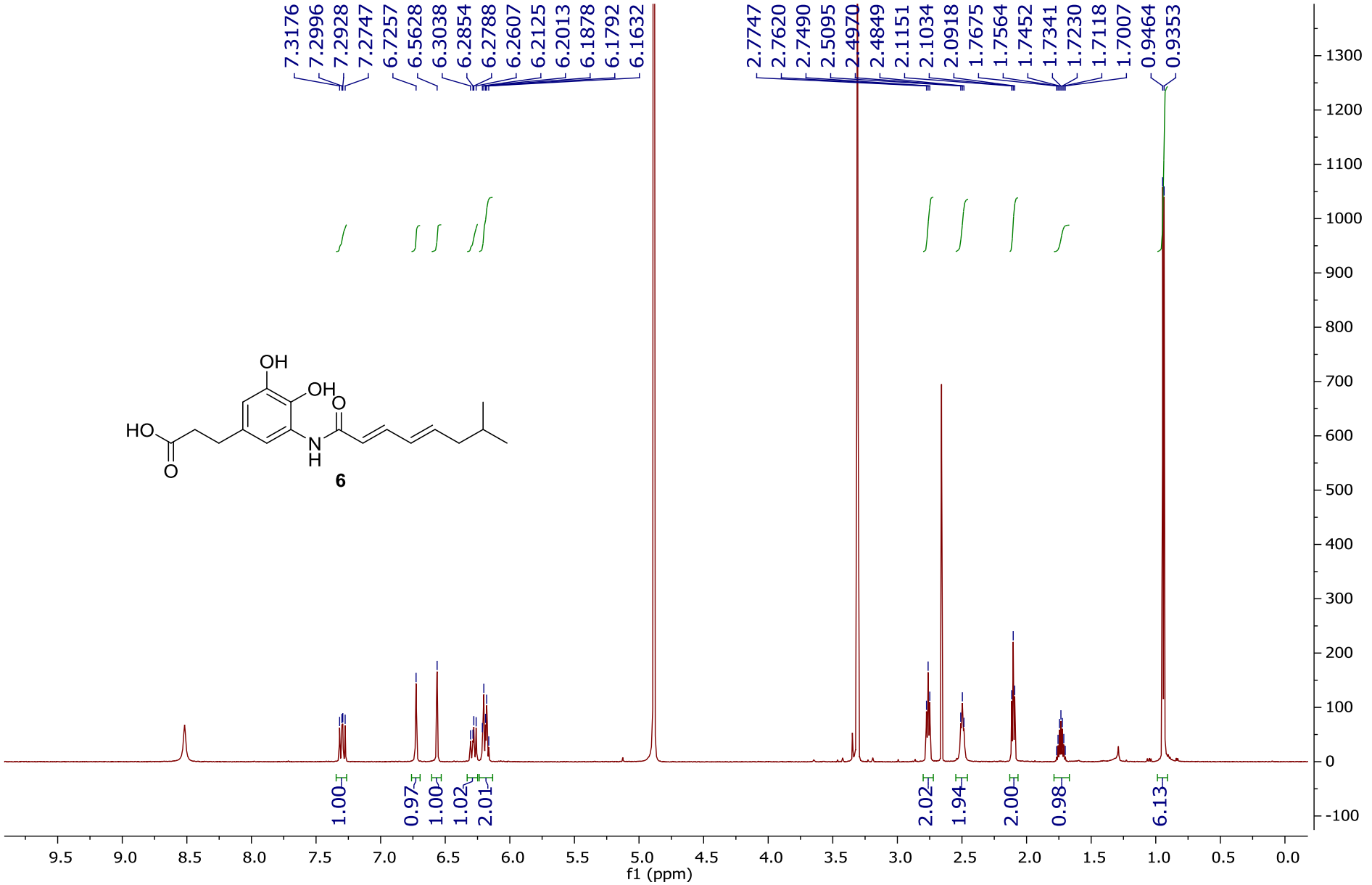

Figure S25. ^{13}C-NMR spectrum of carpatamide G (**6**) in CD_3OD

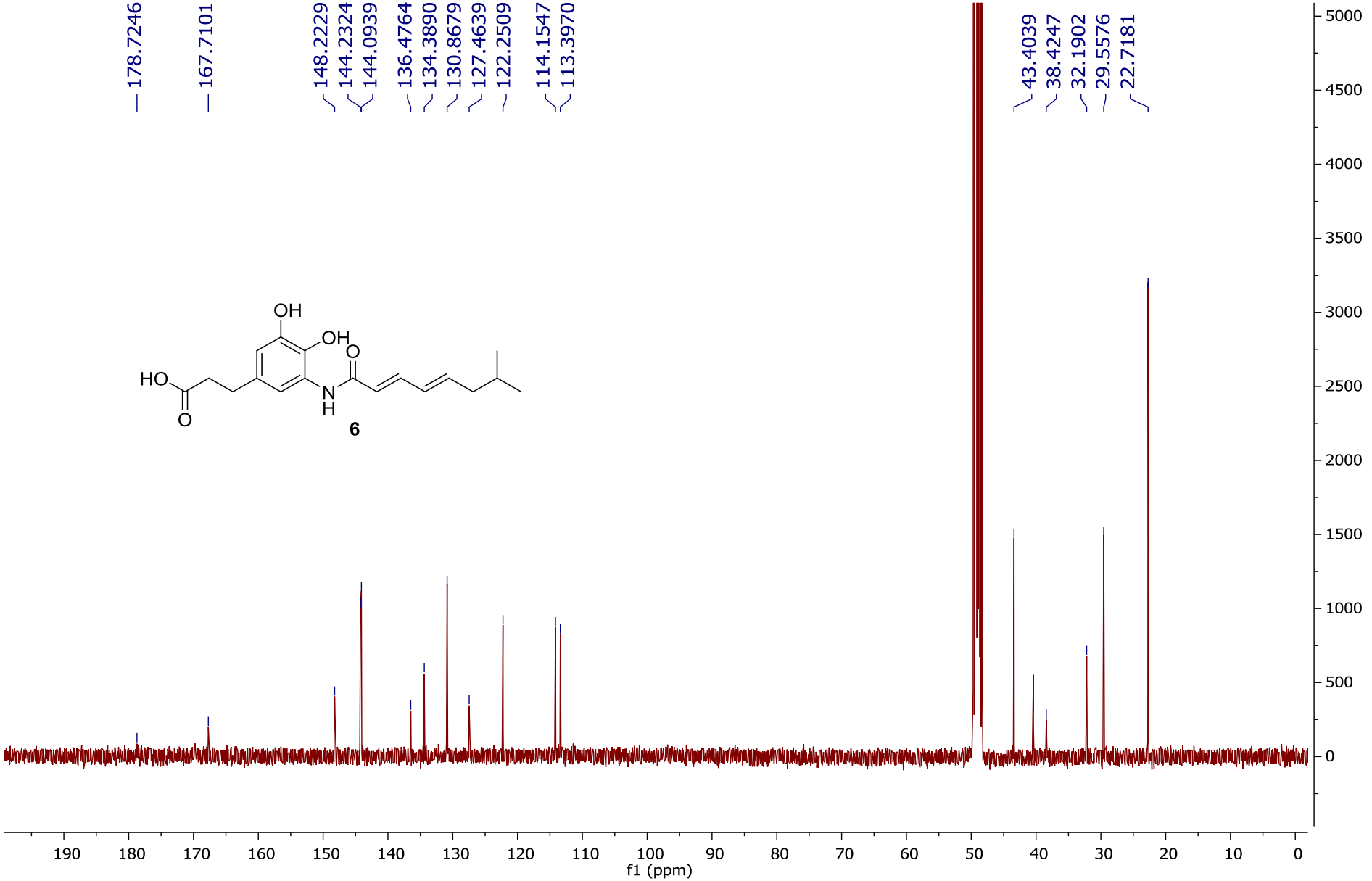

Figure S26. HSQC spectrum of carpatamide G (**6**) in CD_3OD

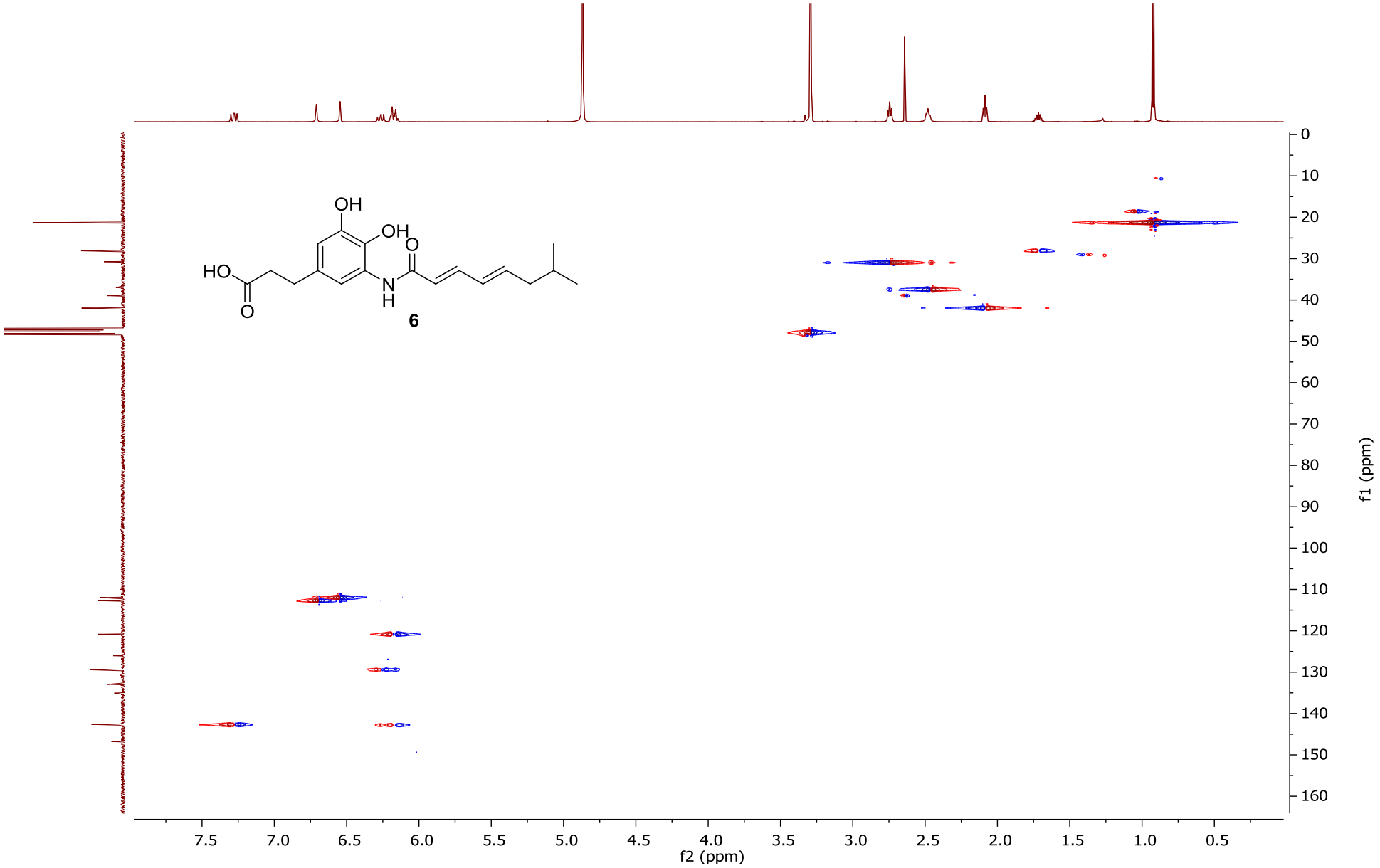

Figure S27. ^{1}H-^{1}H COSY spectrum of carpatamide G (**6**) in CD_3OD

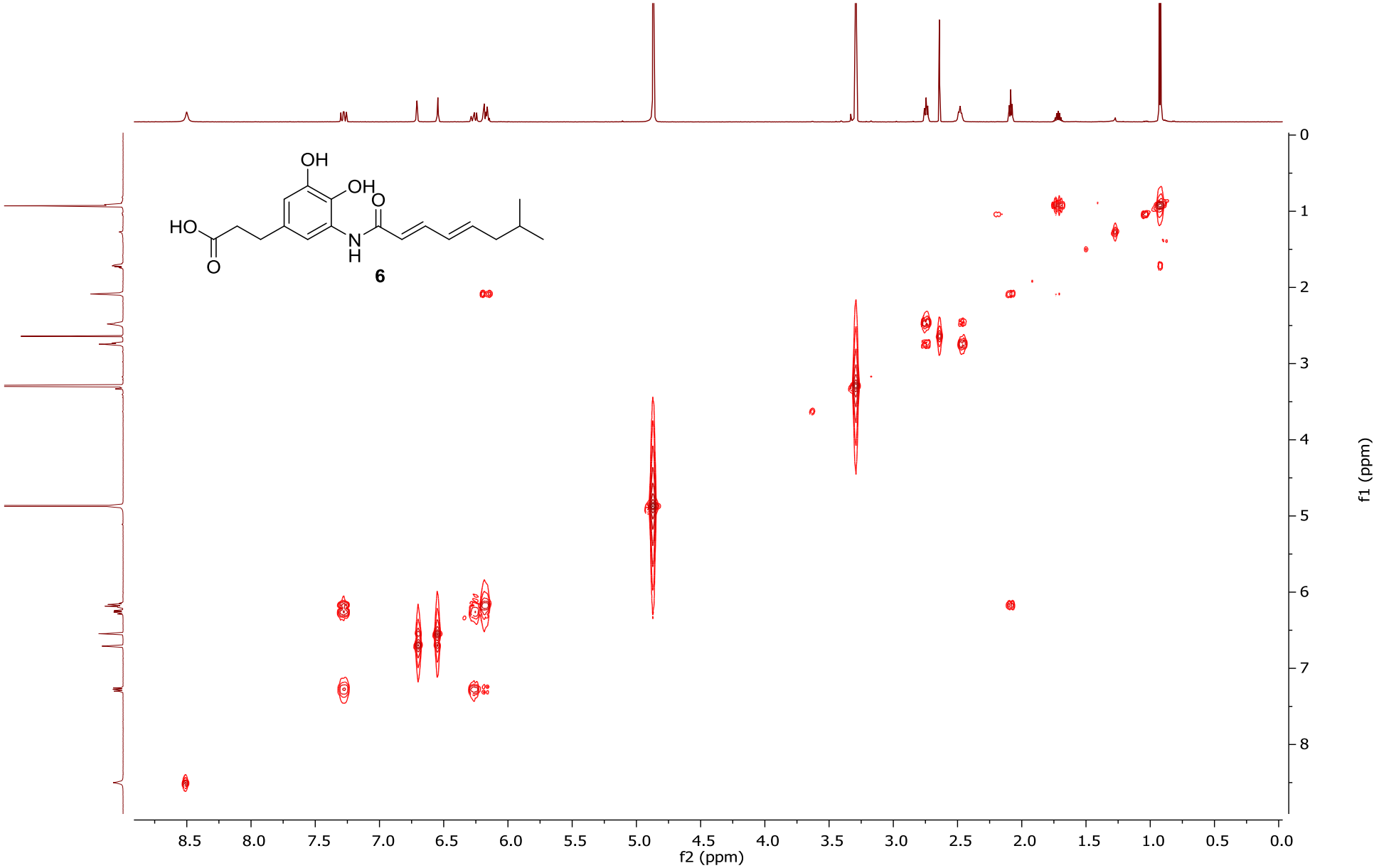

Figure S28. HMBC spectrum of carpatamide G (**6**) in CD_3OD

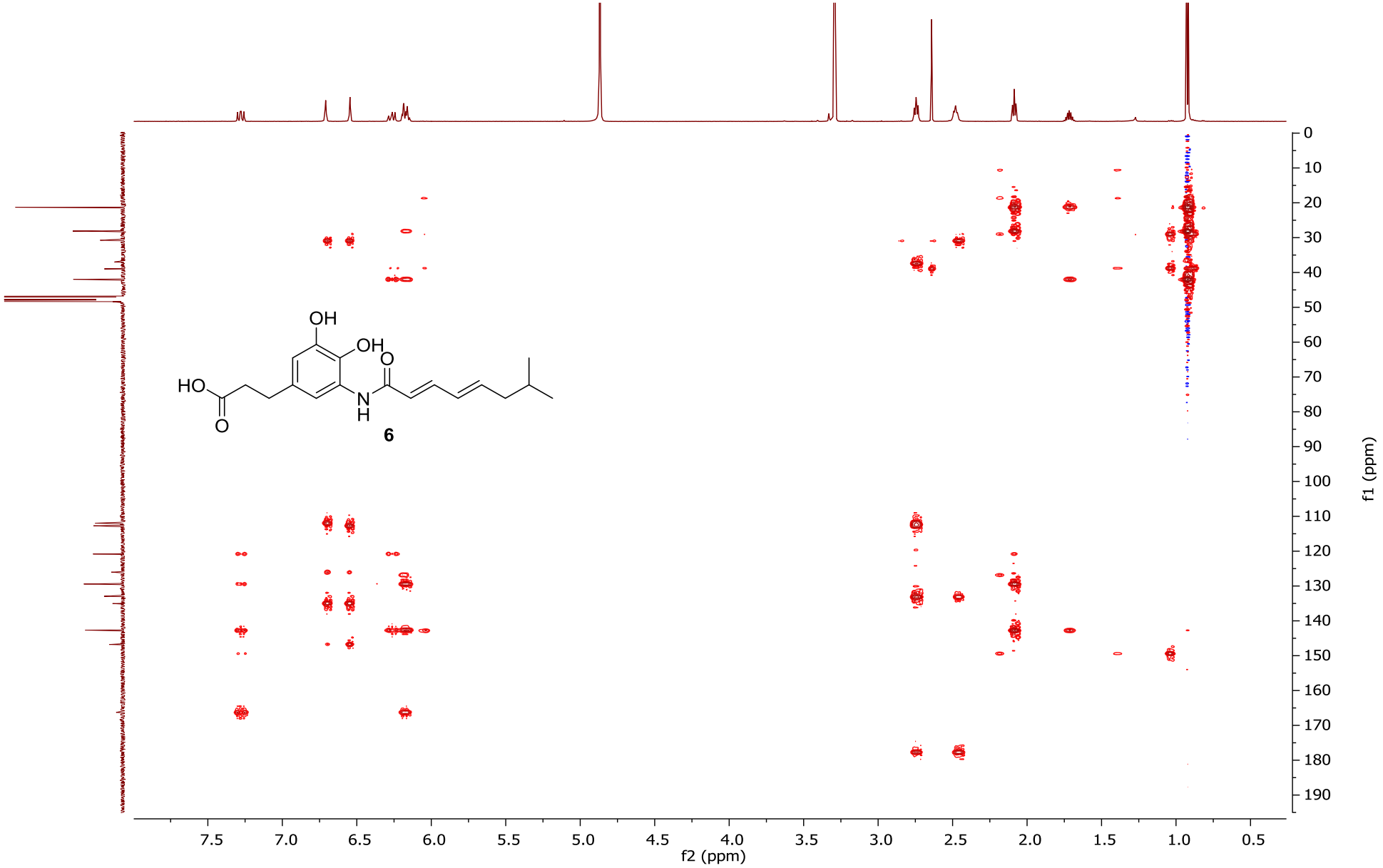

Figure S29. ^{1}H-NMR spectrum of carpatamide H (**8**) in CD_3OD

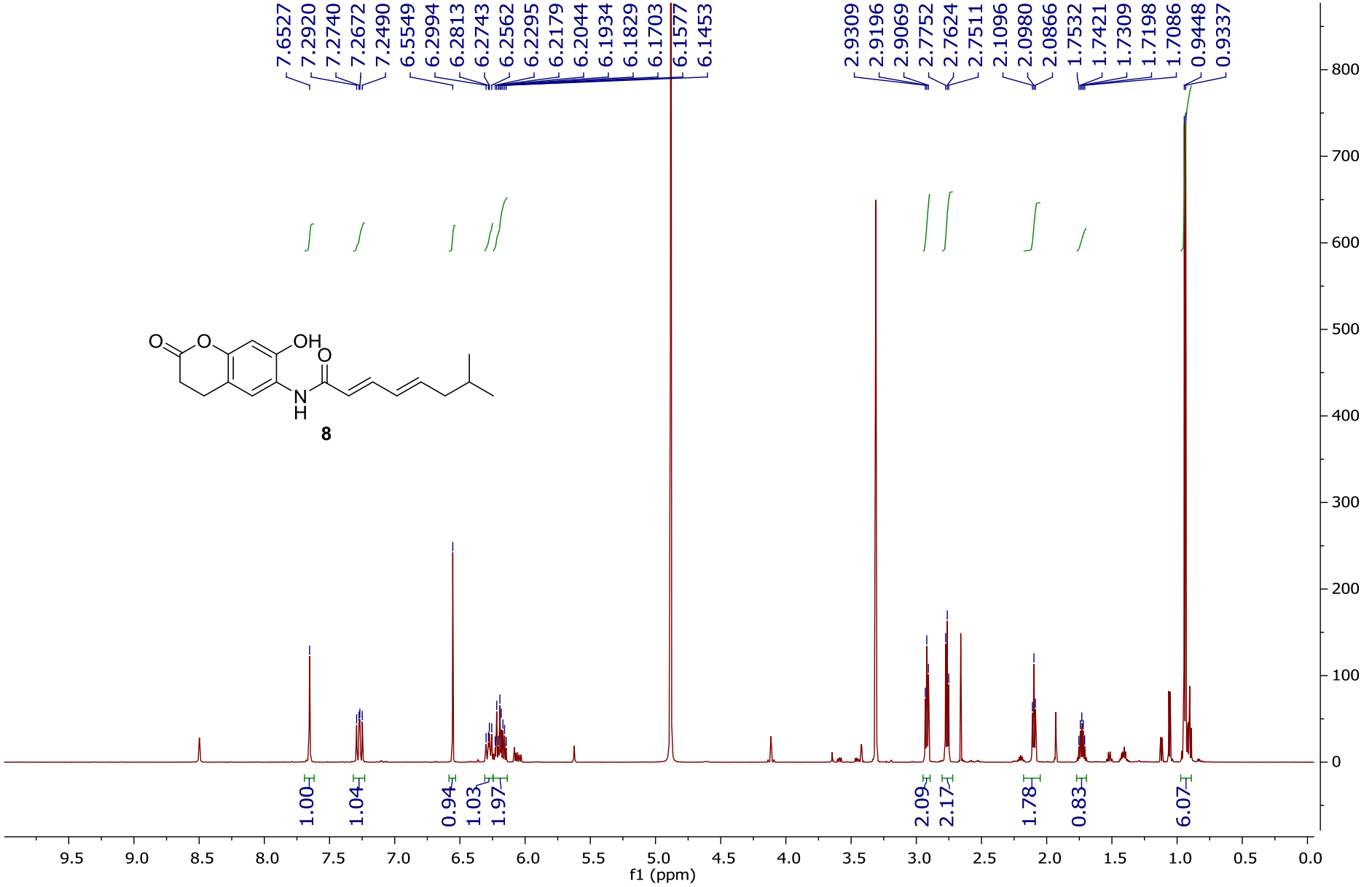

Figure S30. ^{13}C-NMR spectrum of carpatamide H (**8**) in CD_3OD

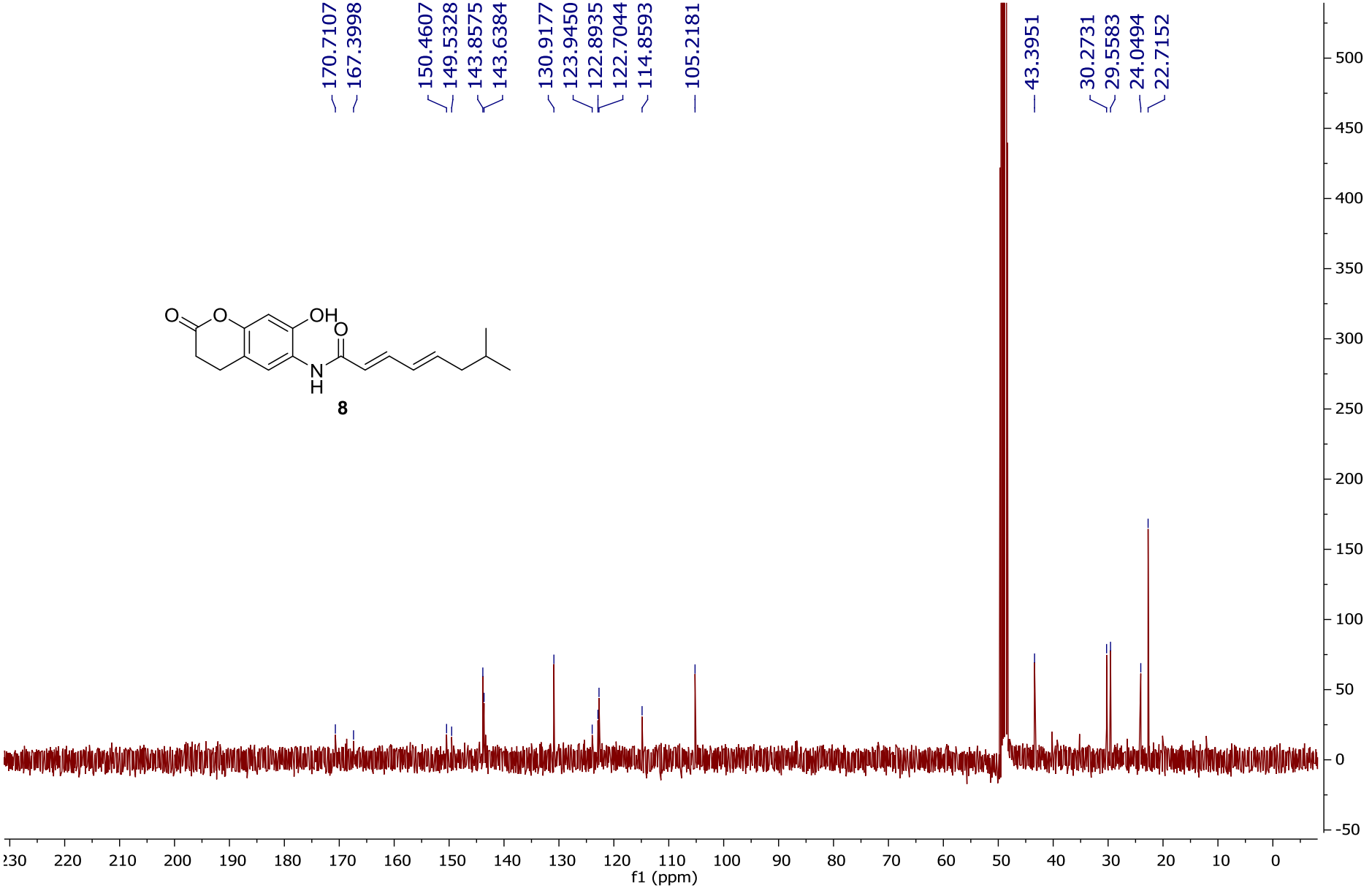

Figure S31. HSQC spectrum of carpatamide H (**8**) in CD_3OD

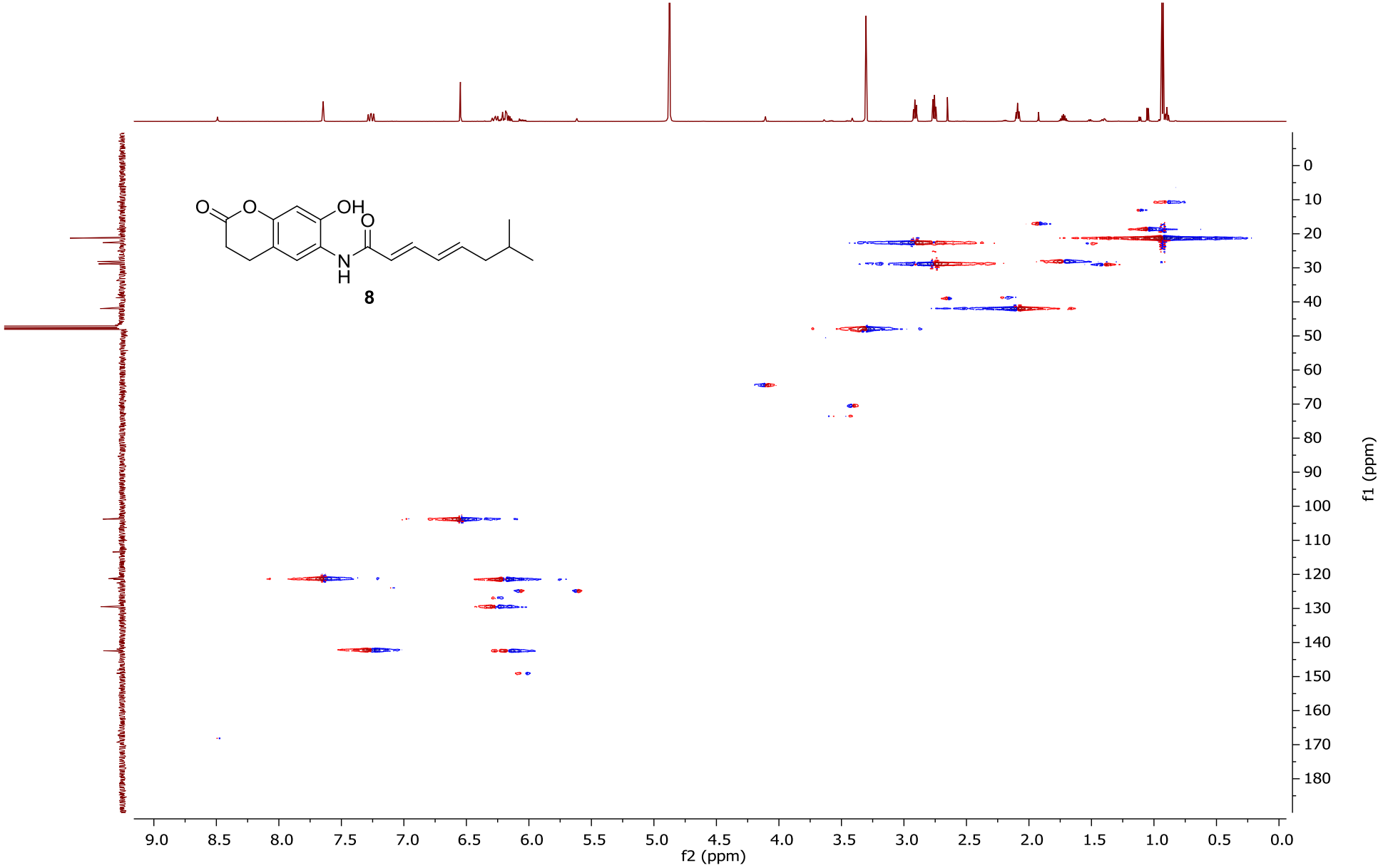

Figure S32. ^{1}H-^{1}H COSY spectrum of carpatamide H (**8**) in CD_3OD

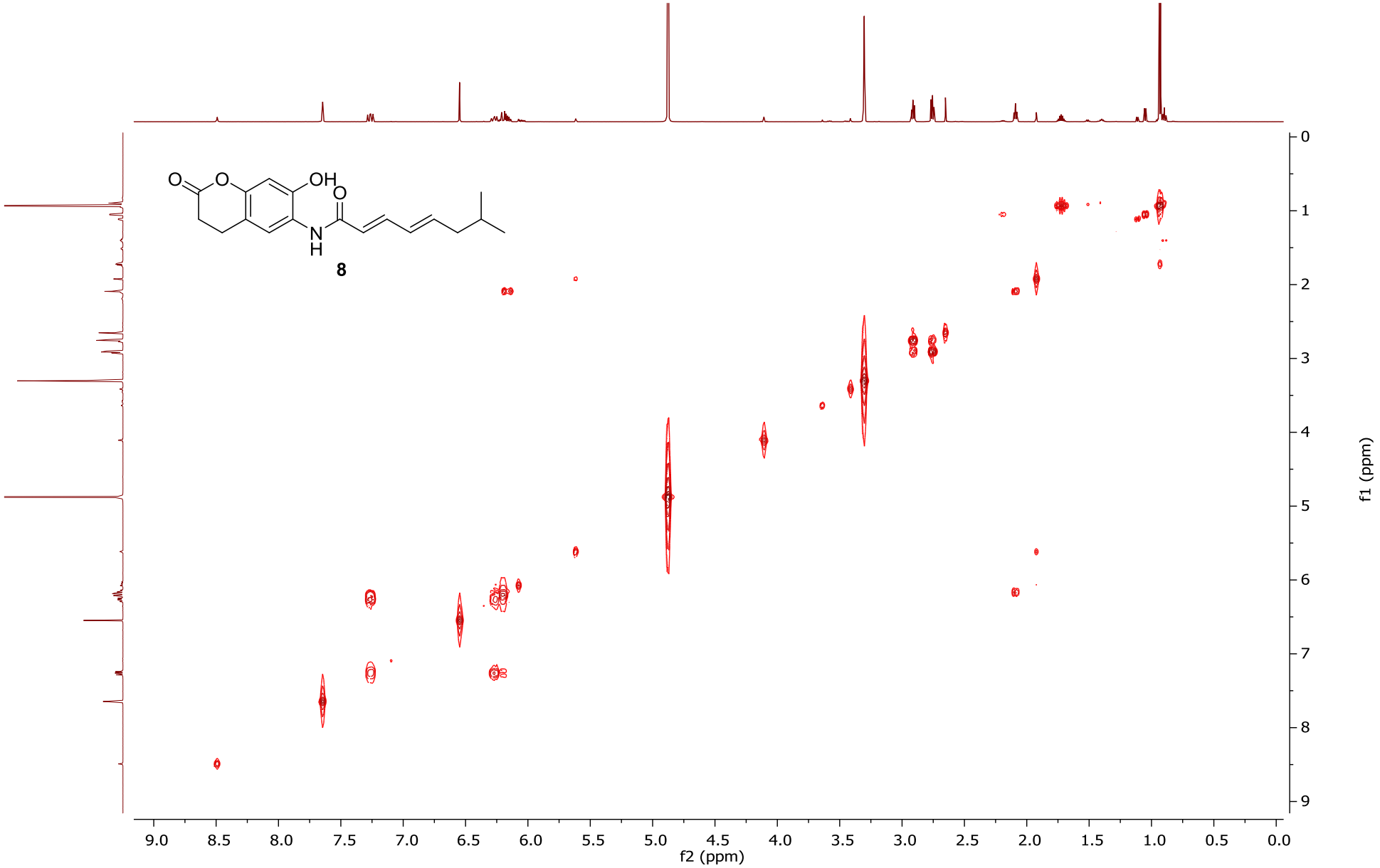

Figure S33. HMBC spectrum of carpatamide H (**8**) in CD_3OD